Pigment Epithelial-Derived Factor Deficiency Accelerates Atherosclerosis Development via Promoting Endothelial Fatty Acid Uptake in Mice With Hyperlipidemia

Haiping Wang, MD;* Yanfang Yang, MS;* Ming Yang, MD; Xinghui Li, PhD; Jing Tan, MD; Yandi Wu, MD; Yuling Zhang, MD, PhD; Yuanlong Li, MD; Bo Hu, PhD; Shijie Deng, MD; Fengmin Yang, BS; Saifei Gao, MS; Hui Li, MS; Zhenyu Yang, BS; Hui Chen, MD, PhD; Weibin Cai, MD, PhD

Background—Endothelial cell injury, induced by dyslipidemia, is the initiation of atherosclerosis, resulting in an imbalance in endothelial fatty acid (FA) transport. Pigment epithelial–derived factor (PEDF) is an important regulator in lipid metabolism. We hypothesized that PEDF is involved in endothelium-mediated FA uptake under hyperlipidemic conditions.

Methods and Results—Circulating PEDF levels were higher in patients with atherosclerotic cardiovascular disease than in normal individuals. However, decreasing trends of serum PEDF levels were confirmed in both wild-type and apolipoprotein E–deficient mice fed a long-term high-fat diet. Apolipoprotein E–deficient/PEDF-deficient mice were generated by crossing PEDF-deficient mice with apolipoprotein E–deficient mice, and then mice were fed with 24, 36, or 48 weeks of high-fat diet. Greater increases in body fat and plasma lipids were displayed in PEDF-deficient mice. In addition, PEDF deficiency in mice accelerated atherosclerosis, as evidenced by increased atherosclerotic plaques, pronounced vascular dysfunction, and increased lipid accumulation in peripheral tissues, whereas injection of adeno-associated virus encoding PEDF exerted opposite effects. Mechanistically, PEDF inhibited the vascular endothelial growth factor B paracrine signaling by reducing secretion of protein vascular endothelial growth factor B in peripheral tissue cells and decreasing expression of its downstream targets in endothelial cells, including its receptors (namely, vascular endothelial growth factor receptor-1 and neuropilin-1), and FA transport proteins 3 and 4, to suppress endothelial FA uptake, whereas PEDF deletion in mice activated the vascular endothelial growth factor B signaling pathway, thus causing markedly increased lipid accumulation.

Conclusions—Decreasing expression of PEDF aggravates atherosclerosis by significantly impaired vascular function and enhanced endothelial FA uptake, thus exacerbating ectopic lipid deposition in peripheral tissues. (*J Am Heart Assoc*. 2019;8:e013028. DOI: 10.1161/JAHA.119.013028.)

Key Words: atherosclerosi • endothelial FA uptake • hyperlipidemia • PEDF • vascular endothelial growth factor B signaling pathway

---

Hyperlipidemia, characterized by excessive plasma lipids, easily induces endothelial injury, which drives and exacerbates atherogenesis.[1–3] Accordingly, excessive liberation of fatty acids (FAs) into the blood results in lipid metabolism disorders and disruptions in the balance of endothelial FA transport.[4,5] As a gatekeeper of FA transport, the endothelium is tightly controlled by complex feedback and feed-forward mechanisms to manipulate energy supply and

<div style="border:1px solid red">

Clinical Perspective

What Is New?

- This study reveals that serum levels of pigment epithelial-derived factor (PEDF) are decreasing in late-stage atherosclerosis with hyperlipidemia, and PEDF deficiency aggravates atherosclerotic plaques, vascular dysfunction, and lipid deposit, whereas PEDF supplement exerts opposite effects under pathological condition of hyperlipidemia.
- PEDF deletion activates vascular endothelial growth factor B signaling pathway to accelerate fatty acid uptake, causing lipid accumulation in peripheral tissues.
- PEDF negatively regulates expressions of vascular endothelial growth factor B from tissue cells, vascular endothelial growth factor B's receptors vascular endothelial growth factor receptor 1 and neuropilin 1, and fatty acid transporter proteins 3/4 on endothelial cells to affect fatty acid uptake.

What Are the Clinical Implications?

- This study provides direct evidence of the role of PEDF in the development of atherosclerosis in response to hyperlipidemia.
- PEDF and vascular endothelial growth factor B–vascular endothelial growth factor receptor 1/neuropilin 1/fatty acid transport proteins 3/4 could act as novel potential therapeutic targets in atherosclerosis.
- We consolidate and complement previous clinical cross-sectional studies that show increasing serum levels of PEDF may be a quick response to metabolic syndrome as a compensatory system in early-stage atherosclerosis.

</div>

demand.[4] The key endothelial signaling molecule, vascular endothelial growth factor B (VEGFB), is involved in the regulation of FA transport.[6,7] VEGFB is highly expressed in adult tissues, including the myocardium, skeletal muscle, and brown adipose tissue, which are involved in paracrine signaling to the vascular endothelium; specifically, VEGFB binds to the endothelial receptor VEGF receptor 1 (VEGFR1) and the coreceptor neuropilin 1 (NRP1) and induces transcriptional upregulation of the vascular-specific FATP3/4 (FA transport proteins 3 and 4) to regulate the transendothelial transport of circulating FAs.[6,8,9] In the pathological condition of dyslipidemia, FA deposition and ectopic lipid accumulation in nonadipose cells suggest that there may be an increase in FA uptake, but the mechanism of endothelium-mediated FA transport remains unclear.

Pigment epithelial-derived factor (PEDF), an endogenously secreted protein that belongs to the serine proteinase inhibitor family, is expressed in multiple tissues.[10–13] Recently, plasma PEDF has been considered a cardiovascular disease (CVD) biomarker because of its association with a variety of metabolic conditions, such as obesity,[14,15] coronary heart disease,[11,16,17] diabetes mellitus,[18,19] and atherosclerosis.[20] Under physiological conditions, PEDF is maintained at a high circulating level to execute its biological activities in lipid metabolism by targeting cells through cell-surface receptors, such as adipose triglyceride lipase.[21–24] Furthermore, PEDF deficiency in mice promotes pancreatic hyperplasia and visceral obesity during pancreatic cancer progression and contributes to the accumulation of lipids in ethanol-induced hepatic steatosis.[25,26] Taken together, these results reveal that PEDF may be involved in FA transport in adiposity. In addition, PEDF ameliorates endothelial injury and reduces oxidative stress by suppressing the Wnt/β-catenin pathway induced by oxidized low-density lipoprotein (LDL) and reducing vascular permeability.[27–29] However, further studies need to be done to address the role of circulating PEDF in the late stage of progressive atherosclerosis and whether PEDF is involved in modulating endothelial FA transport under hyperlipidemic conditions.

In this study, we combined clinical research with animal models of 2 genotypes of mice (wild type [WT] and apolipoprotein E deficient [ApoE$^{-/-}$]) fed a long-term high-fat diet (HFD) to observe PEDF expression characteristics. In addition, the current study investigated whether PEDF deficiency in ApoE$^{-/-}$ mice, induced by hyperlipidemia, aggravates endothelial dysfunction and atherosclerotic plaque formation using ApoE$^{-/-}$/PEDF-deficient (PEDF$^{-/-}$) and ApoE$^{-/-}$ mice fed with HFD for 24, 36, or 48 weeks; we also examined whether overexpression of PEDF in ApoE$^{-/-}$/PEDF$^{-/-}$ mice exerts opposite effects. Then, the signaling pathway responsible for lipid accumulation in peripheral tissues in PEDF-deficient mice in late-stage atherosclerosis and the mechanism of PEDF regulation of endothelial FA uptake were investigated using in vitro experiments.

Methods

The data that support the findings of this study are available from the corresponding author on reasonable request.

Study Population

A total of 228 participants (128 patients and 100 healthy controls) who were admitted to the Department of Cardiology of Sun Yat-sen Memorial Hospital underwent coronary angiography from January 2010 to June 2016. Among those who participated in this study, 128 subjects were diagnosed as having atherosclerotic CVD (ASCVD) and dyslipidemia. According to the criteria of the 2007 Chinese Joint Committee for Developing Chinese Guidelines on Prevention and Treatment of Dyslipidemia in Adults,[30] dyslipidemia was diagnosed if a patient had the following characteristics: (1) fasting triglyceride of ≥1.7 mmol/L or receipt of specific treatment

for previously diagnosed hypertriglyceridemia; and (2) fasting high-density lipoprotein cholesterol (HDL-C) of <1.04 mmol/L or receipt of specific treatment for previously diagnosed low HDL-C level. Patients with serious hepatic or renal dysfunction were excluded. All enrollees were given written informed consent for participation in this study and finished a standardized questionnaire to self-report past and present illnesses, medications, and smoking habits. The study was approved by the ethical committees of Sun Yat-sen Memorial Hospital and Sun Yat-sen University.

Animal Experiments

All animal experiments were performed in accordance with approved protocols of the Sun Yat-sen University Animal Care and Use Committee and are in line with the *Guide for the Care and Use of Laboratory Animals* of the National Institute of Health in China. Double-knockout mice (ApoE$^{-/-}$/PEDF$^{-/-}$) were generated by crossbreeding of PEDF-deficient mice on a C57BL/6J background (kindly provided by Prof Guoquan Gao, Sun Yat-sen University) with ApoE$^{-/-}$ mice also on a C57BL/6J background (originally purchased from the Jackson Laboratory). We determined the genotypes of double-knockout mice by polymerase chain reaction (PCR) analysis using genomic DNA extracted from mouse tails. Genotyping for the ApoE locus was done according to the protocol provided by the Jackson Laboratory with the use of the following primers (Table S1). A 155-bp amplified fragment is from the WT locus, whereas a 245-bp fragment is from the targeted allele. PEDF-KO genotyping was conducted by the primers (Table S1) with a 350-bp fragment from the WT locus and a 500-bp fragment from the targeted allele (Figure S1A). Double-knockout mouse genotype was further confirmed by Western blot analysis by using commercially available antibodies against PEDF (Abcam, Cambridge, UK) (Figure S1B). Moreover, serum PEDF levels were measured in age-matched male WT, ApoE-KO, and double-knockout mice fed with standard chow diets (CDs) for 8 weeks (Figure S1C).

Male ApoE$^{-/-}$/PEDF$^{-/-}$ mice, aged 6 to 8 weeks, were randomly grouped and then placed on HFD (D12492, consisting of fat [60%], protein [20%], and carbohydrate [20%]; all from Guangdong Medical Laboratory Animal Center, Guangzhou, China) for 24, 36, or 48 weeks. Age- and sex-matched ApoE$^{-/-}$/PEDF$^{+/+}$ and WT mice were put on either CD or HFD for 12, 24, 36, or 48 weeks. All mice were housed in a 12-hour light/dark cycle and had access to food and water ad libitum. Mice were fasted for 6 hours before euthanasia.

Cell Culture

Human umbilical vein endothelial cells (HUVECs) (kindly provided by Prof Hui Chen, Sun Yat-sen Memorial Hospital) were cultured in Human Endothelial-SFM supplemented with 10% fetal bovine serum, 10 μg/mL heparin, 250 ng/mL EGF (epidermal growth factor), and 500 ng/mL basic fibroblast growth factor [all from Thermo Fisher Scientific, Waltham, MA). Cells were used between passages 3 and 6 in all the experiments. C2C12 cells (purchased from Institute of Biochemistry and Cell Biology, CAS (Chinese Academy of Sciences), China] were grown in DMEM supplemented with 10% fetal bovine serum, 100 U/mL penicillin G, and 100 μg/mL streptomycin. At ≈85% to 90% confluence, myoblast differentiation was induced by differentiation medium (DMEM supplemented with 4% horse serum) for 3 to 4 days. Mouse aortic smooth muscle cells were cultured in DMEM with 10% fetal bovine serum. All cells were incubated at 37°C in a humidified 5% CO_2 incubator.

Isolation and Culture of Neonatal Mouse Cardiomyocytes

Neonatal mouse cardiomyocytes were isolated from 1- to 2-day-old WT mice on a C57BL/6J background. Hearts were removed, then ventricles were pooled, and cells were dispersed by successive enzymatic digestion with pancreatin (0.5 mg/mL; Thermo Fisher Scientific) and collagenase II (0.4 mg/mL; Thermo Fisher Scientific). Cell suspension was thereafter purified by centrifugation through differential adhesion method to obtain myocardial cell cultures with 99% myocytes. After seeding on 6-well plates coated with gelatin (0.2% in PBS; Sigma-Aldrich, St Louis, MO), neonatal mouse cardiomyocytes were cultured in DMEM supplemented with 10% horse serum and placed in 37°C-5% CO_2 atmosphere. After 24 hours, ≈95% of the cells displayed spontaneous contractile activity in culture. Then, cells were cultured in serum-free medium for 12 hours before treatment.

Plasma Characterization

Mouse blood samples were collected from anesthetized mice. After standing for 20 minutes, blood samples were centrifuged at 400*g* for 20 minutes at 4°C to separate plasma. Distributions of total cholesterol (TC), triglyceride, free FAs, high-density lipoprotein cholesterol, and LDL cholesterol in plasma were measured using commercial enzymatic kits. For more details, please see Table S2.

Micron-Scale Computed Tomography Analysis

Mice were anaesthetized with 5% isoflurane. Transverse micron-scale computed tomography images of the whole abdomen were scanned using a micron-scale computed tomography scanner (Inveon PET/CT, Germany). Three-dimensional images of each mouse were reconstructed using Inveon Research Workplace V2 software. The amount of

subcutaneous adipose tissue in mice was measured using Image J software.[31]

Mouse Atherosclerotic Lesion Measurements

Mice were euthanized, and aortas were collected from the base of ascending aorta to the iliac bifurcation. Aortas were split longitudinally, pinned onto flat black silicone plate, and then fixed in 4% formaldehyde in PBS overnight. Fixed aortas were stained with oil red O for 4 hours, washed with PBS briefly, and digitally photographed at a fixed magnification. Images were captured with Leica microscope (Leica DFC550 Microsystems, Wetzlar, Germany) at a $\times 5$ magnification, and quantification was performed with Image J software. Transverse sections of aortic arch were cut at 10-µm thickness every 100 µm, according to methods in previous studies.[32,33] Each section was stained with oil red O for 20 minutes and then dyed with hematoxylin. The quantification was performed with Image-Pro Plus 6.0 software.

Intravenous Injections of Adeno-Associated Virus

Adeno-associated virus (AAV) vectors (serotype 2/9) were constructed and packaged by Hanbio Biotechnology (Shanghai, China). These AAV vectors contained either null insertion of green fluorescent protein (GFP) (AAV-GFP; used as control) or cDNA insertion encoding full length of mouse WT PEDF (AAV-PEDF). To maintain the titer of AAV, 6- to 8-week-old male ApoE$^{-/-}$/PEDF$^{-/-}$ mice were fed with HFD for 20 weeks, and then injected with 1.2×10^{11} vg of AAV-GFP (AAV-GFP injected mice; n=8) or AAV-PEDF (AAV-PEDF injected mice; n=10) through the tail vein. ApoE$^{-/-}$/PEDF$^{-/-}$ mice were taken as controls. After injections, 3 groups of mice were fed with additional 4 months of HFD (Figure S2A).

Vascular Function

Mice were euthanized, and then the entire aortas were removed carefully and placed in ice-cold Krebs solution. After careful clearance of adipose tissue, artery segments (3–4 mm) were cannulated with 2 pressure probes of isolated vascular tensiometer (DMT 620M; Denmark) and suspended in the Krebs-filled chambers, which were aerated with 95% O_2 and 5% CO_2 and maintained at a temperature of 37°C. Then, the vessels were equilibrated for 2 hours. After equilibration, arterial viability was assessed by stimulation with a dose of saturated KCl solution. After washing and stabilization to baseline, cumulative concentration-response curves were generated by adding increasing concentrations (10^{-9}–10^{-5} mol/L) of acetylcholine after preconstriction with concentration of 10 µmol/L 5-hydroxytryptamine creatinine sulfate complex. Then, vessels were preincubated with 10^{-4} mol/L N^G-nitro-L-arginine methyl ester, hydrochloride for 30 minutes, and then concentrations (10^{-9}–10^{-5} mol/L) of acetylcholine and (10^{-10}–10^{-5} mol/L) of sodium nitroprusside were added in order. The percentage vasodilation was calculated from the preconstricted internal diameter and the dilated diameter at a given concentration, such that % [BD (baseline diameter)−Preconstricted Internal Diameter]/Vasodilation=[(Dilated Diameter−Preconstricted Internal Diameter)] $\times 100$. All drugs were purchased from Sigma-Aldrich.

Blood Pressure Recordings

Arterial blood pressure (BP) was measured by the intelligent noninvasive tail cuff system (BP-2010E; Beijing, China) following the manufacturer's protocol. Systolic BP, diastolic BP, and mean BP as well as heart rate were recorded. Briefly, BP measurements (technical replicates) were taken in mice; all false readings (as determined by the diagnostic software) were excluded, and any animal failing to register at least 20 (80%) true readings was excluded from analysis. A total of 30 measurements were obtained and averaged for each mouse. BP was calculated through BP-2010 series software.

Oil Red O and Hematoxylin Staining

Tissues were placed in 4% paraformaldehyde for 12 hours. Then, 15% and 30% sucrose gradients were dehydrated for 1 day, and tissues were embedded in O.C.T gel until the tissues completely sank to the bottom. Cryosections (10 µm) were mounted onto the microscope slides and air dried for 2 hours. Sections were rinsed with 60% isopropanol for 2 to 5 minutes and then stained for neutral lipid content using Oil Red O (Sigma-Aldrich) for 10 to 15 minutes (liver sections for 10 minutes, heart and muscle sections for 15 minutes). After washing with distilled water, the nuclei were stained with hematoxylin for 45 seconds. Sections were visualized through Leica Microsystems at $\times 200$ and $\times 400$ magnifications.

Enzyme-Linked Immunosorbent Assays

Human serum samples were collected. Then, the PEDF and VEGFB levels were assayed by ELISA using Human PEDF DuoSet ELISA kits (R & D Systems, Minneapolis, MN) and Human VEGFB ELISA Kit (Sigma-Aldrich). PEDF levels in the mouse serum were measured using a mouse PEDF ELISA kit (USCN Business Co, Ltd, Wuhan, China), according to the instructions provided by manufacturers.

Western Blot Analysis

Cells were lysed by ice-cold radioimmunoprecipitation assay buffer (Beyotime, Shanghai, China). Tissues were

homogenized in radioimmunoprecipitation assay buffer supplemented with protease, phosphatase, and kinase inhibitors. Proteins were measured with the BCA Protein assay kit (Millipore, Billerica, MA), resolved by PAGE bis-tris electrophoresis, and transferred onto polyvinylidene difluoride membranes (Millipore). Proteins were probed with the following primary antibodies: rabbit anti-PEDF (1/1000; ab180711; Abcam), rabbit anti-VEGFR1 (1/1000; ab32152; Abcam), rabbit anti-NRP1 (1/1000; ab81321; Abcam), rabbit anti-FATP3 (1/1000; ab123104; Abcam), rabbit anti-FATP4 (1/1000; ab199719; Abcam), and rabbit anti-GAPDH (1/5000; D16H11; CST, MA). Bound antibodies were detected with enhanced-chemiluminescence detection reagent (Millipore). The protein intensity was detected, quantified, and normalized to that of GAPDH by using a ChemiDoc imaging system (Bio-Rad Laboratories, Hercules, CA) and Image J software. All experiments were repeated at least 3 times.

4,4-Difluoro-3A,4Adiaza-S-Indacene Uptake Assay

HUVECs were starved for 6 to 8 hours before different treatments for 24 hours as follows: (1) 100 nmol/L PEDF protein (gift from Prof Guoquan Gao); (2) 100 nmol/L VEGFB protein (ab179970; Abcam); (3) a mixture of 100 nmol/L PEDF protein and 100 nmol/L VEGFB protein; or (4) mixtures of 100 nmol/L PEDF protein and 100 nmol/L VEGFB protein plus 2 μg/mL PEDF neutralizing antibodies (gift from Prof Guoquan Gao). Then, HUVECs were cultured in growth medium containing 1% BSA and 50 μmol/L 4,4-difluoro-3a,4adiaza-s-indacene (BODIPY)–C16 (Life Technologies, Carlsbad, CA) for 30 minutes at 37°C. Cells were collected and washed by 1× PBS–1% FF-BSA 3 times, and then fixed by 4% paraformaldehyde at room temperature for 15 minutes. Images were captured using Leica TCS-SP2-AOBS confocal microscope with ×20 objective and equal exposure times. Three-well repeats were performed for each experiment.

The BODIPY-FA uptake experiment was adopted as previously described.[34] BODIPY-C16 was resuspended in 1 mL 1× PBS containing 0.1% dimethyl sulfoxide and then diluted with 1% BSA in 0.1 μg/μL BODIPY-C16 work solution. WT, ApoE$^{-/-}$, and ApoE$^{-/-}$/PEDF$^{-/-}$ mice with 24-week HFD were fasted for 8 hours and then injected with 0.5 μg BODIPY-C16 per gram of body weight via the tail vein. Controls were injected equal volume of 1× PBS–1% BSA. After injection for 0.5 or 1 hour, the tissues of mice were harvested and observed using Top-Quality Digital Camera Technology (Leica DFC550, Germany).

Pulse Wave Velocity Measurements

To assess large-artery stiffening, aortic pulse wave velocity (PWV) was measured by using Mouse Doppler Instruments (INDUS, Webster, TX). Mice were anesthetized under 2%

isoflurane in the Matrx anesthesia system (Midmark, New York, NY) for 1 to 2 minutes. Anesthesia was maintained via nose cone, and mice were secured in a supine position on a heating board (≈37°C) to maintain body temperature. Velocity spectrogram acquisitions were completed at the aortic arch and the abdominal aorta by using 2 probes (20-Hz probes) and analyzed through Doppler Signal Processing Workstation. Absolute pulse arrival times were indicated by the recorded ECG (electrocardiogram) signals. PWV was calculated by using the separation distance and pulse arrival time: PWV (cm/s)=[Distance (cm)/Time (s)].

Quantitative Reverse Transcription–PCR Analysis

Tissues from male mice fed with 24 weeks HFD were dissected, frozen, and stored at −80°C. Whole tissue RNA was isolated with RNAiso Plus reagents (Takara Bio, Otsu, Japan), according to manufactures' instructions. Total RNA (1 μg) was reverse transcribed using PrimeScript RT Reagent Kit with gDNA Eraser (Takara). Quantitative reverse transcription–PCR was performed with SYBR Premix Ex Taq II (Takara) and 20 ng cDNA per reaction. Primer sequences are listed in Table S3. Quantitative reverse transcription–PCR was performed by QuantStudio 6 Flex system (Life Technologies).

In Vivo Ultrasound Imaging for Flow Measurements

To evaluate the local ascending and descending aortic flow velocity in mice correlated with the atherosclerotic distribution and plaque burden, a high-frequency ultrasound scanner (Vevo 2100; Visual Sonics, Toronto, ON, Canada) with a 30-MHz transducer was used. After 2.5% isoflurane anesthesia via a mask, Doppler flow spectra were recorded at different levels and made at 3 locations: (1) the region close to the greater curvature (outer radius), (2) the middle lumen, and (3) the region close to the lesser curvature (inner radius) for ascending aorta example. With an ECG-triggering function, consecutive Doppler color flow images of the local flow velocity across the aortic lumen and their dynamic changes through the cardiac cycle can be obtained. The transducer orientation was carefully adjusted to make the Doppler intercept angle as small as possible, and all the velocity measurements were angle corrected. In no measurement did the intercept angle exceed 60°.

Immunostaining

After treatments, HUVECs were fixed by 4% paraformaldehyde at room temperature for 15 minutes immediately and treated with 0.1% Triton for 10 minutes. Cells were blocked by 5% goat serum and incubated with primary antibodies of rabbit anti-

VEGFR1 (1/250; ab32152; Abcam) or rabbit anti-NRP1 (1/250; ab81321; Abcam), which were colocalized with mouse anti-CD31 (1/100; ab24590; Abcam) overnight at 4°C. Goat anti-rabbit IgG cross-adsorbed secondary antibody Alexa Fluor 594 (1/500; A-11012; Thermo Fisher Scientific) and goat anti-mouse IgG cross-adsorbed secondary antibody Alexa Fluor 488 (1/500; A-11001; Thermo Fisher Scientific) were mixed and incubated at 37°C for 1.5 hours and then for next experiments. Images were captured using Leica TCS-SP2-AOBS confocal microscope with ×20 objective and equal exposure times. Three-well repeats were performed for each experiment.

Hearts were collected and then fixed by 4% paraformaldehyde at 4°C overnight and then sucrose gradient dehydration was performed. Tissues were cryosectioned into 6-μm sections. Immunostaining of VEGFR1 or NRP1 colocalized with CD31 in hearts was performed by using antibodies of anti-VEGFR1, anti-NRP1, and anti-CD31 (Abcam). These quantifications were done on 3 fields per section (n=3–4 mice per genotype). Immunolocalization of FATP3,FATP4, and VEGFB in paraffin sections of hearts was performed by using the following primary antibodies of goat anti-FATP3 (sc-137235; Santa Cruz Biotechnology, Santa Cruz, CA), rabbit anti-FATP4 (ab199719; Abcam), and rabbit anti-VEGFB (ab185696; Abcam). Sections were stained with hematoxylin before analysis by bright-field microscopy.

Statistical Analysis

Data are expressed as mean±SEM, whereas clinical results are displayed as mean±SD. Comparisons between participants with and without ASCVD were performed using a χ^2 test for categorical variables and the Student t test for continuous variables. Correlation between circulating serum levels of PEDF and VEGFB were analyzed with Pearson correlation. Multivariate stepwise regression analysis was used to further assess the clinical variables correlated with serum PEDF. ANOVA with a Dunnett's test was used for comparing multiple groups, and a Bonferroni's test was applied when making multiple pair-wise comparisons between different groups. All analyses were considered statistically significant at $P<0.05$.

Results

Plasma PEDF Develops Dynamic Variations in Atherosclerosis Progression

The baseline characteristics of the enrolled participants, including 128 patients with ASCVD and dyslipidemia and 100 normal subjects with non-ASCVD, are summarized in Table. Compared with non-ASCVD subjects, patients with ASCVD showed significantly higher SBP and DBP levels, in addition to changes in serum levels of MetS (metabolic syndrome)–defining parameters, including higher fasting glucose, TC, triglyceride, LDL cholesterol, free FAs, and high-sensitivity CRP (C-reactive protein) levels and lower serum HDL-C levels. The serum PEDF level was significantly higher in subjects with ASCVD than in those without ASCVD (15.64±5.32 versus 13.60±4.27 μg/mL; Figure 1A). In addition, characteristics of circulating PEDF levels were observed in WT mice fed a long-term HFD. We previously observed that plasma PEDF levels continued to increase in WT mice as the duration of HFD feeding increased from 4 to 12 weeks compared with

Table. Clinical Characteristics and Biochemical Parameters Between 2 Groups

Variables	ASCVD	Non-ASCVD	*P* Value
No.	128	100	
Age, y	64.3±12.3	61.2±11.2	0.093
Sex (men/women)	77:51	51:49	0.167
BMI, kg/m^2	24.7±2.88	23.0±2.49	0.103
Systolic blood pressure, mm Hg	134.4±19.4	125.7±11.5	0.003
Diastolic blood pressure, mm Hg	82.8±8.3	78.1±8.86	0.009
Fasting glucose, mmol/L	5.63±1.79	4.93±0.77	<0.001
Total cholesterol, mmol/L	4.95±1.10	4.37±0.69	<0.001
Triglycerides, mmol/L	2.13±1.47	1.36±0.86	<0.001
HDL cholesterol, mmol/L	0.95±0.21	1.22±0.31	<0.001
LDL cholesterol, mmol/L	3.21±0.86	2.89±0.71	0.003
hs-CRP, mg/L	1.96 (0.56–6.66)	1.25 (0.08–4.61)	0.008
Free fatty acids, μmol/L	501.1±215.6	436.0±177.6	0.015

Data are expressed as mean±SD, unless otherwise indicated. ASCVD indicates atherosclerotic cardiovascular disease; BMI, body mass index; HDL, high-density lipoprotein; hs-CRP, high-sensitivity C-reactive protein; LDL, low-density lipoprotein.
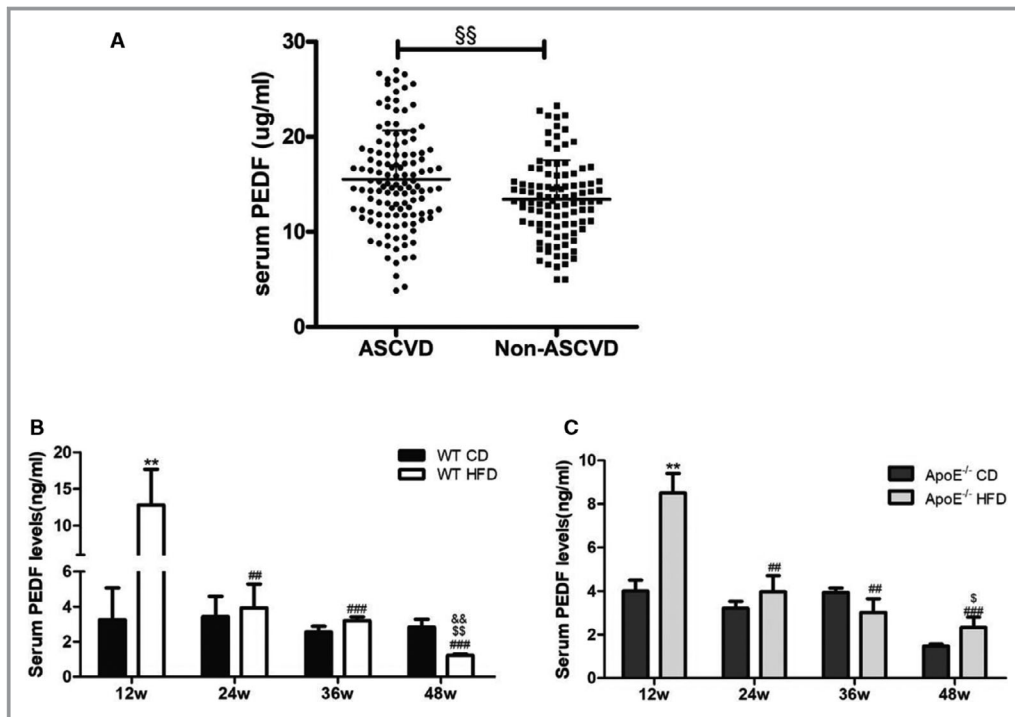
Figure 1. Serum pigment epithelial-derived factor (PEDF) levels in humans and mice. **A**, ELISA analysis of serum PEDF levels in participants with and without atherosclerotic cardiovascular disease (ASCVD). ELISA analysis of serum PEDF levels in wild-type (WT) (**B**) and apolipoprotein E–deficient (ApoE$^{-/-}$) (**C**) mice fed a high-fat diet (HFD) for 12, 24, 36, or 48 weeks compared with WT or ApoE$^{-/-}$ mice with a chow diet (CD) (per group, n=5–7). Data are presented as mean±SD. $^{§§}P<0.01$, ASCVD vs non-ASCVD; $^{**}P<0.01$ HFD and CD; $^{##}P<0.01$, $^{###}P<0.001$ vs 12 weeks HFD; $^{$}P<0.05$; $^{$$}P<0.01$ vs 24 weeks HFD; $^{&&}P<0.01$ vs 36 weeks HFD.

those in mice fed CD, which is in accordance with the previous literature.[35] Interestingly, circulating PEDF levels had a decreasing trend in mice after 12 to 24 weeks of HFD. For further study, we extended the HFD induction period. Age-matched male WT and ApoE$^{-/-}$ mice were selected and fed either HFD or CD for 12, 24, 36, or 48 weeks. Serum levels of PEDF were decreased in WT mice after 12 to 48 weeks of HFD, whereas no difference was shown in WT mice fed CD (Figure 1B). Moreover, a similar reduction in plasma PEDF levels was detected in ApoE$^{-/-}$ mice fed HFD (Figure 1C). Additional serum biochemical characteristics of WT mice and ApoE$^{-/-}$ mice are shown in Tables S4 through S6.

PEDF Deficiency Accelerates Atherosclerotic Plaque Formation

To establish the active involvement of PEDF in the development of atherosclerosis, we generated double-knockout mice (ApoE$^{-/-}$/PEDF$^{-/-}$) by crossbreeding PEDF knockout mice with ApoE-deficient mice (Figure S1A through S1C). Then, ApoE$^{-/-}$/PEDF$^{-/-}$, ApoE$^{-/-}$, and WT mice were fed HFD for 24, 36, or 48 weeks. Age-matched WT mice fed normal CD served as controls.

HFD-induced weight gain was significantly higher in ApoE$^{-/-}$/PEDF$^{-/-}$ mice than in ApoE$^{-/-}$ mice and WT mice fed HFD for 24 and 36 weeks, but no difference was observed for ApoE$^{-/-}$ mice fed HFD for 48 weeks, probably because of the long induction time and old age (Figure 2A). Furthermore, epididymal fat pad weights in ApoE$^{-/-}$/PEDF$^{-/-}$ mice were significantly increased compared with those in the other 3 groups after 24, 36, or 48 weeks of HFD (Figure 2B). Accordingly, micron-scale computed tomography whole-body scan analyses showed remarkably increased visceral and subcutaneous fat in ApoE$^{-/-}$/PEDF$^{-/-}$ mice after 24 weeks of HFD (Figure 2C). The serum biochemical characteristics of the 4 groups of mice are shown in Tables S4 through S6. Moreover, significant increases or increasing trends for serum lipid parameters, including triglyceride, TC, free FAs, fasting blood glucose, and LDL cholesterol levels, and lower circulating HDL-C levels, were detected in the absence of PEDF in mice. These findings suggested that hyperlipidemia appeared earlier in ApoE$^{-/-}$/PEDF$^{-/-}$ mice. The extent of atherosclerotic lesions, as measured by en face staining with oil red O, was increased by 1.52 ($P<0.01$), 1.73 ($P<0.05$), and 1.47 ($P<0.05$) fold in the aortas of ApoE$^{-/-}$/PEDF$^{-/-}$ mice
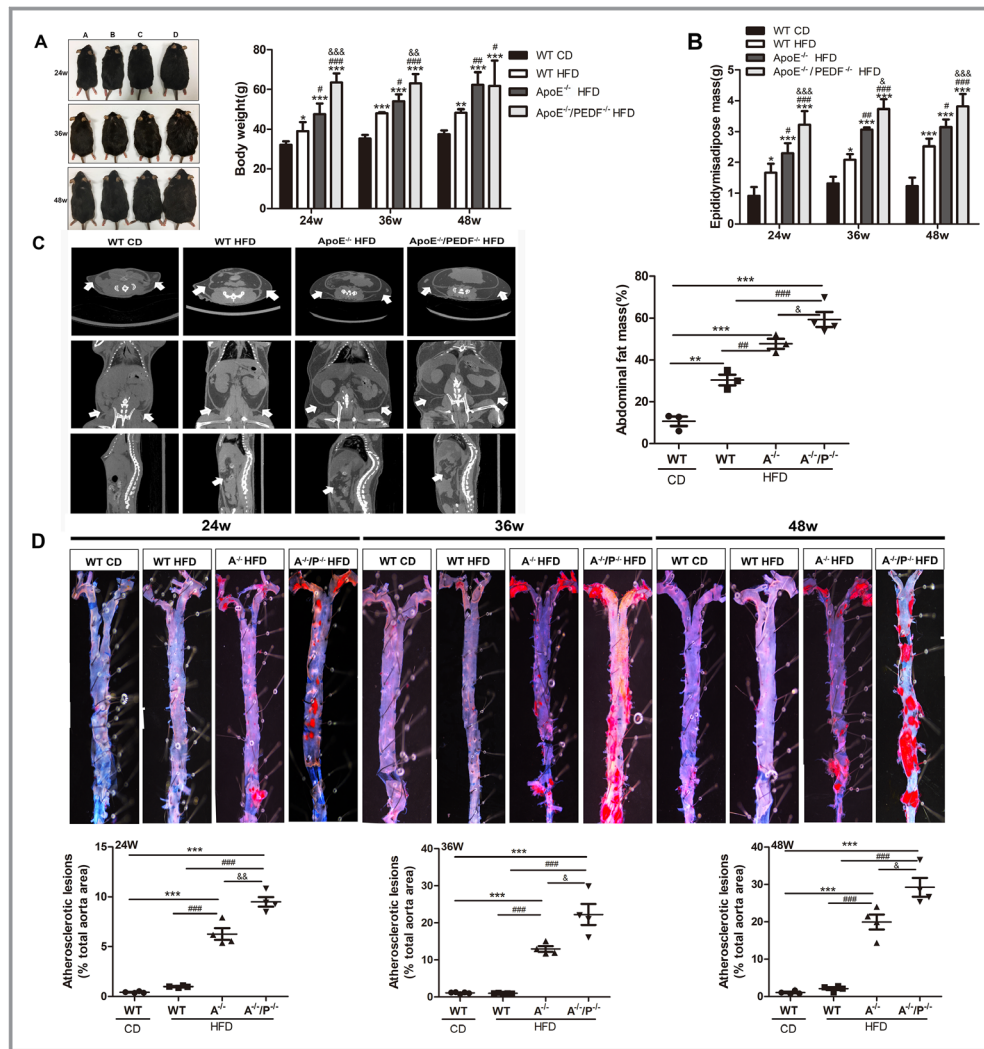
Figure 2. Pigment epithelial–derived factor (PEDF) deficiency accelerates atherosclerosis. **A**, Representative images of mice (A, wild type and chow diet [WT CD]; B, WT and high-fat diet [HFD]; C, apolipoprotein E deficient [ApoE$^{-/-}$] and HFD; and D, ApoE$^{-/-}$/PEDF deficient [PEDF$^{-/-}$] and HFD) (left); body weight (**A**, right) and epididymal fat pad mass (**B**) were measured in WT, ApoE$^{-/-}$, and ApoE$^{-/-}$/PEDF$^{-/-}$ mice fed HFD for 24, 36, or 48 weeks and age-matched WT fed CD (per group, n=4–7). **C**, Representative images of micron-scale computed tomography (left) and their quantification (right) of the abdominal and subcutaneous fat (per group, n=3–4). The blank signal with white arrows represents adipose tissues. **D**, Representative images of intraluminal surface of the total aorta stained with oil red O; red plaque covered area was assessed and expressed as percentage of total area (below images) (per group, n=4–5). **E**, Representative images of cross-sections of aortic arch (left) and quantifications (right) (per group, n=3–7) (bar=2 μm). Data are presented as mean±SE. *$P<0.05$, **$P<0.01$, ***$P<0.001$ vs WT CD; #$P<0.05$, ##$P<0.01$, ###$P<0.001$ vs WT HFD; &$P<0.05$, &&$P<0.01$, &&&$P<0.001$ vs ApoE$^{-/-}$ HFD.

compared with ApoE$^{-/-}$ mice after 24, 36, and 48 weeks of HFD, respectively (Figure 2D). In addition, the percentages of plaques in the ascending regions of the aortic arch were significantly higher in ApoE$^{-/-}$/PEDF$^{-/-}$ mice than in ApoE$^{-/-}$ mice (23.95%±1.5% versus 12.57%±3.76% [$P<0.001$], 31.62%±3.94% versus 18.1%±4.12% [$P<0.05$], and 48.89%±6.62% versus 26.73%±3.46% [$P<0.01$], respectively) (Figure 2E).

AAV-PEDF Injection Slows the Formation of Atherosclerotic Plaques in ApoE$^{-/-}$/PEDF$^{-/-}$ Mice

To investigate whether PEDF supplementation could reverse atherosclerotic plaque formation, 6- to 8-week-old male ApoE$^{-/-}$/PEDF$^{-/-}$ mice were fed HFD for 20 weeks and were then injected with either AAV encoding PEDF (AAV-PEDF) or AAV encoding GFP (AAV-GFP). After AAV injection, ApoE$^{-/-}$/
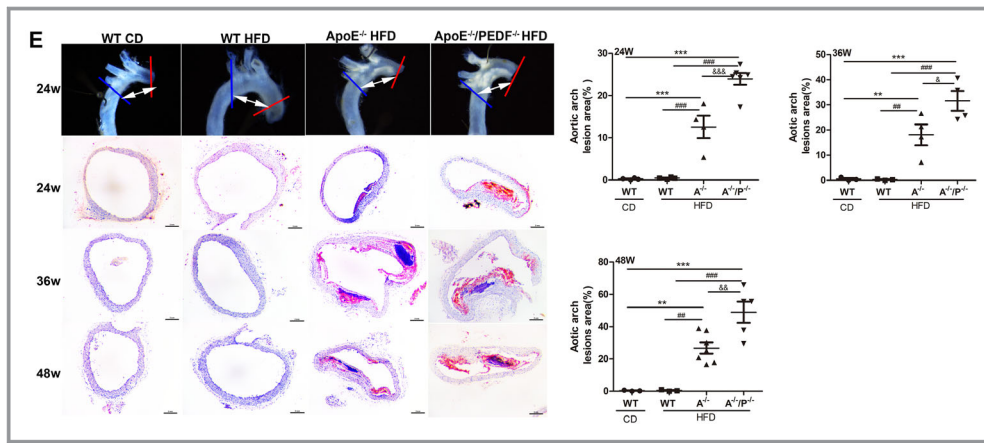
Figure 2. Continued

PEDF$^{-/-}$ mice were fed HFD for an additional 16 weeks (Figure S2A). Age- and sex-matched ApoE$^{-/-}$/PEDF$^{-/-}$ mice with no AAV injection served as blank controls. After 36 weeks of HFD, PEDF expression was assessed in adipose tissues and livers, which are the main sources of circulating PEDF.[10,13] Images of adipose tissues and livers revealed strong fluorescence intensity in the AAV-injected mice (Figure S2B). As indicated by Western blotting, PEDF expression in adipose tissues and livers in AAV-PEDF mice exceeded that in AAV-GFP and AAV-control mice by >50% (Figure S2C). A remarkable reduction in body weight was observed in AAV-PEDF mice compared with that in AAV-GFP and AAV-control mice (Figure 3A). Similarly, an obvious decrease in epididymal fat pad mass was detected in AAV-PEDF mice (Figure 3B). Micron-scale computed tomography images showed significant reductions in visceral and subcutaneous fat in AAV-PEDF mice (Figure 3C). In addition, lower serum levels of TC, triglyceride, free FAs, fasting blood glucose, and LDL cholesterol and a higher serum level of HDL-C were observed in AAV-PEDF mice relative to those in the other 2 groups (Table S7). Moreover, en face analysis of aortas stained with oil red O showed that atherosclerotic lesions were markedly decreased in AAV-PEDF mice compared with those in AAV-GFP and AAV-control mice after 36 weeks of HFD (18.0%±2.83% versus 34.2%±2.30% versus 35.2%±1.7%; $P<0.05$) (Figure 3D). Accordingly, atherosclerotic plaques in AAV-PEDF mice were significantly decreased in the ascending regions of the aortic arch (18.11%±0.65% versus 33.1%±2.36% versus 31.3%±2.84%; $P<0.001$) (Figure 3E).

PEDF Significantly Ameliorates Vascular Function in the Hyperlipidemic State

To further determine the effect of PEDF deficiency on vascular function, vascular parameters were measured in the 6 groups of mice (WT CD, WT HFD, ApoE$^{-/-}$ HFD, ApoE$^{-/-}$/PEDF$^{-/-}$ HFD, AAV-PEDF HFD and AAV-GFP HFD). Tail-cuff SBP values were significantly higher in ApoE$^{-/-}$/PEDF$^{-/-}$ mice than in ApoE$^{-/-}$ mice and WT mice after 24, 36, or 48 weeks of HFD (Figure 4A), whereas SBP values in AAV-PEDF mice were conversely reduced compared with those in AAV-GFP and AAV-control mice after 36 weeks of HFD (Figure S3A). The DBP and mean BP values were both significantly increased in ApoE$^{-/-}$/PEDF$^{-/-}$ mice at 24 or 36 weeks of HFD but were similar compared with those of the other groups at 48 weeks of HFD (Figure 4B and 4C). After AAV delivery, DBP and mean BP were markedly lower in AAV-PEDF mice than in AAV-GFP and AAV-control mice (Figure S3B and S3C). To examine aortic stiffness, aortic PWV measurements were obtained using a Doppler-based device. An obvious elevation in PWV was observed in ApoE$^{-/-}$/PEDF$^{-/-}$ mice at 24, 36, or 48 weeks of HFD compared with that in ApoE$^{-/-}$ and WT mice (Figure 4D), whereas a dramatic decrease in PWV and an improvement in vascular function were shown in AAV-PEDF mice (Figure S3D). We then tested the ascending and descending aorta blood velocity using a high-frequency ultrasound scanner to examine arterial compliance and hemodynamics. The peak blood velocity was clearly increased in ApoE$^{-/-}$/PEDF$^{-/-}$ mice at different HFD induction times (Figure 4E and 4F), whereas AAV-PEDF injection ameliorated arterial compliance (Figure S3E and S3F). Furthermore, endothelium-dependent vasodilation was dramatically impaired in ApoE$^{-/-}$/PEDF$^{-/-}$ mice in response to acetylcholine induction of dose-dependent relaxation in contrast to that in ApoE$^{-/-}$ and WT mice after 36 weeks of HFD (Figure 4G). On treatment with N^{G}-nitro-L-arginine methyl ester, hydrochloride (10^{-4} mol/L; an NO synthase inhibitor) for 30 minutes, no difference in endothelium-dependent vasodilation was found among the 4 groups (Figure 4H). The relaxation in response to sodium nitroprusside (an NO donor) did not differ across all groups (Figure 4I).
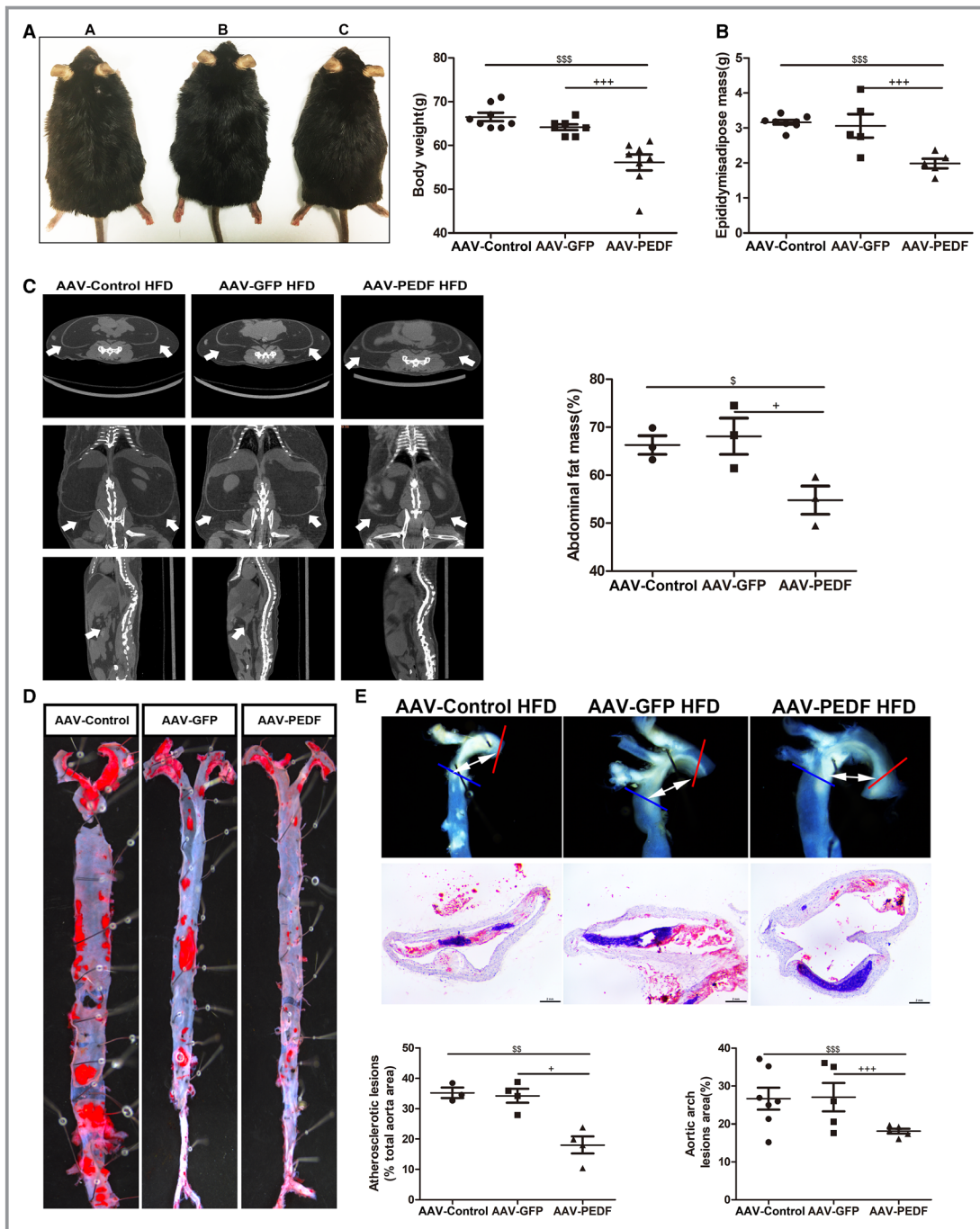
Figure 3. The adeno-associated virus (AAV)–pigment epithelial-derived factor (PEDF) injection in apolipoprotein E–deficient/PEDF-deficient mice slows atherosclerotic plaque formation. **A**, Representative images of mice (A, AAV-control; B, AAV–green fluorescent protein [GFP]; C, AAV-PEDF) (left); body weight (**A**, right) and epididymal fat pad mass (**B**) were measured in AAV-control, AAV-GFP, and AAV-PEDF mice fed high-fat diet (HFD) for 36 weeks (per group, n=7–8). **C**, Representative images of micron-scale computed tomography (left) and their quantification (right) of the abdominal and subcutaneous fat (per group, n=3). The blank signal with white arrows represents adipose tissues. **D**, Representative images of intraluminal surface of the total aorta stained with oil red O; red plaque covered area was assessed and expressed as percentage of total area (right) (per group, n=3–4). **E**, Representative images of cross-sections of aortic arch and quantifications (below images) (per group, n=4–7) (bar=2 μm). Data are presented as mean±SE. $^{\$}P<0.05$, $^{\$\$}P<0.01$, $^{\$\$\$}P<0.001$ vs AAV-control HFD; $^{+}P<0.05$, $^{+++}P<0.001$ vs AAV-GFP HFD.
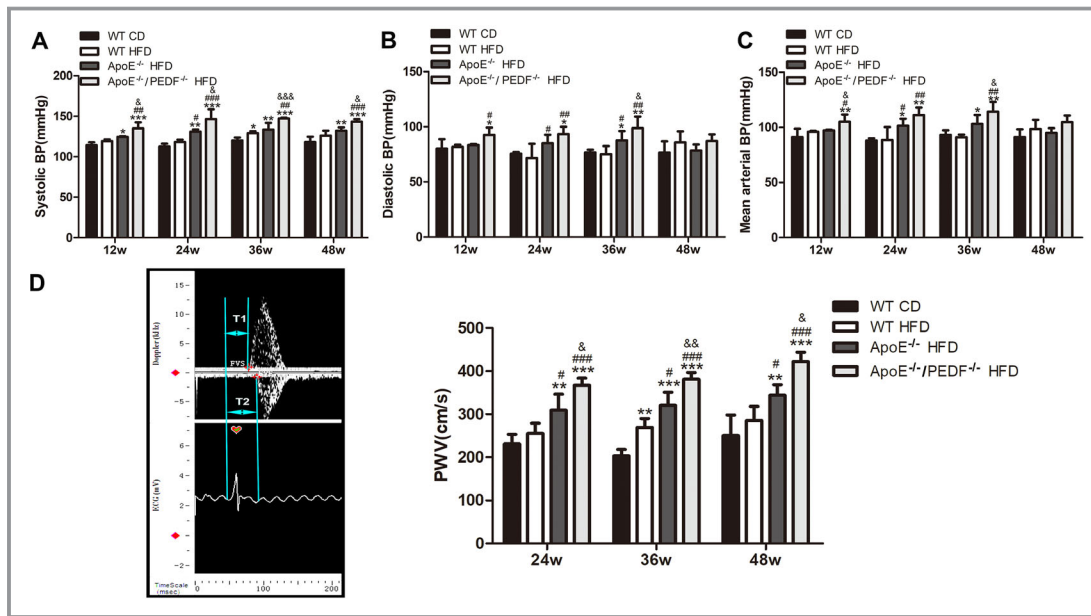
Figure 4. Pigment epithelial-derived factor (PEDF) significantly improves vascular function in condition of hyperlipidemia. Systolic blood pressure (**A**), diastolic blood pressure (**B**), and mean arterial blood pressure (**C**) were measured in wild-type (WT) (chow diet [CD]), WT, apolipoprotein E–deficient (ApoE$^{-/-}$), and ApoE$^{-/-}$/PEDF-deficient (PEDF$^{-/-}$) mice fed high-fat diet (HFD) for 12, 24, 36, or 48 weeks (per group, n=6–10). Aortic stiffness was assessed by pulse-wave velocity (representative PAGE [left] and quantification [right]; **D**), ascending aortic peak velocity (**E**), and descending aortic peak velocity (**F**) in each group of mice (representative images [top] and quantification [bottom]) after 24, 36, or 48 weeks of HFD (per group, n=4–6). **G**, Cumulative concentration-response curve to acetylcholine (10^{-9}–10^{-6} mol/L). **H**, Cumulative concentration-response curve to acetylcholine (10^{-9}–10^{-6} mol/L) after treatment with N^G-nitro-L-arginine methyl ester, hydrochloride (L-NAME) (10^{-4} mol/L) for 30 minutes. **I**, Cumulative concentration-response curve to sodium nitroprusside (SNP) (10^{-10}–10^{-6} mol/L) was measured in WT, ApoE$^{-/-}$, and ApoE$^{-/-}$/PEDF$^{-/-}$ mice fed HFD for 24 weeks and age-matched WT fed CD (per group, n=4–5). Data are presented as mean±SE. *$P<0.05$, **$P<0.01$, ***$P<0.001$ vs WT CD; #$P<0.05$, ##$P<0.01$, ###$P<0.001$ vs WT HFD; &$P<0.05$, &&$P<0.01$, &&&$P<0.001$ vs ApoE$^{-/-}$ HFD.

PEDF Deficiency Aggravates Lipid Deposition in Peripheral Tissues

To identify the effect of PEDF deficiency on lipid metabolism, oil red O staining was applied to investigate the lipid distribution in peripheral tissues, including the liver, heart, and skeletal muscle of mice, at 24, 36, or 48 weeks of HFD. Compared with the other mice, HFD-induced PEDF-deficient mice exhibited the prominent appearance of lipid droplets in the liver, heart, and skeletal muscle (Figure 5A, 5C, and 5E). Similarly, we found that the lipid concentrations of triglyceride and TC in the liver, heart, and skeletal muscle were all significantly higher in ApoE$^{-/-}$/PEDF$^{-/-}$ mice than in ApoE$^{-/-}$ and WT mice (Figure 5B, 5D, and 5F). In contrast, dramatic decreases in lipid accumulation in the liver, heart, and skeletal muscle were observed in AAV-PEDF mice compared with those in AAV-GFP and AAV-control mice after 36 weeks of HFD (Figure 5G). In addition, the concentrations of triglyceride and TC in the liver, heart, and skeletal muscle were all obviously reduced in AAV-PEDF mice (Figure 5H).

These findings collectively suggest that PEDF has a conserved role in lipid homeostasis.

PEDF Deletion Activates VEGFB Signaling in Hyperlipidemic Conditions

The increase in lipid accumulation in peripheral tissues could be largely attributed to the increase in FA uptake in ApoE$^{-/-}$/PEDF$^{-/-}$ mice. Thus, green fluorescent FA (Bodipy FL C$_{16}$) uptake experiments were performed in vivo.[34] The results showed that ApoE$^{-/-}$/PEDF$^{-/-}$ mice had a much greater ability to take in FA analogs in peripheral tissues than other mice (Figure 6A). There is emerging evidence that 2 key genes of the VEGFB and peroxisome proliferator-activated receptor γ signaling pathways can directly target the endothelium to maintain lipid homeostasis.[6] Thus, we analyzed the transcriptional levels of FATP3, FATP4, VEGFR1, NRP1, peroxisome proliferator-activated receptor γ, and FA translocase (Cd36) in hearts from ApoE$^{-/-}$/PEDF$^{-/-}$, ApoE$^{-/-}$, and WT mice at
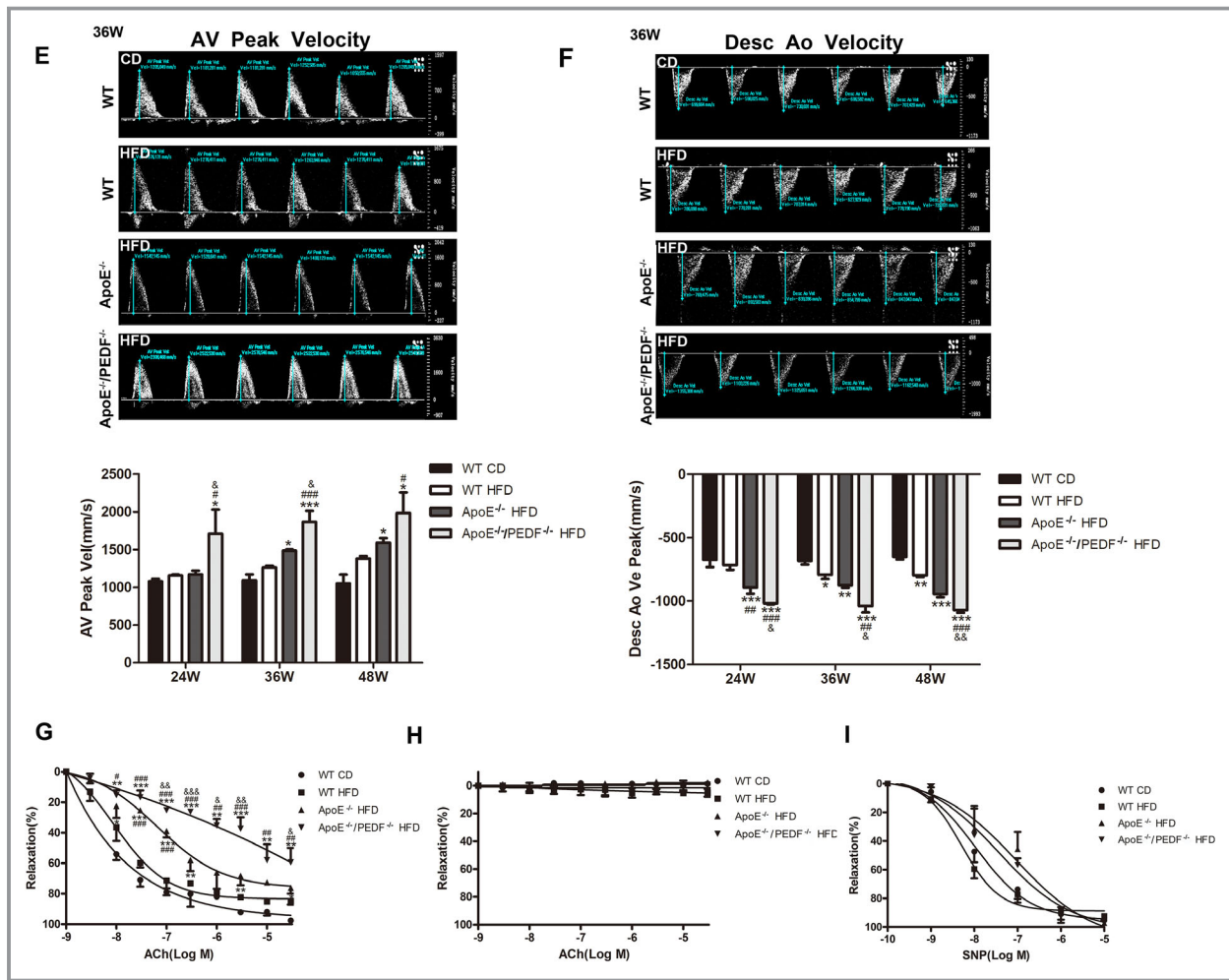
Figure 4. Continued

24 weeks of HFD and in hearts from WT mice at 24 weeks of CD. CD36 expression was downregulated in both $ApoE^{-/-}$/$PEDF^{-/-}$ and $ApoE^{-/-}$ mice, whereas peroxisome proliferator-activated receptor γ expression was clearly upregulated, probably because it was activated by the complex response mechanism of the body to the pathological condition of endothelial dysfunction.[36] FATP4, a vascular-specific target gene of the VEGFB signaling pathway, was remarkably higher in $ApoE^{-/-}$/$PEDF^{-/-}$ mice than in $ApoE^{-/-}$ and WT mice. Minor increases in FATP3, VEGFR1, and NRP1 expression were detected in $ApoE^{-/-}$/$PEDF^{-/-}$ mice (Figure 6B). The consistent increasing trend of key genes involved in the VEGFB signaling pathway suggested that the regulation of endothelial FA transport by PEDF expression might be related to the VEGFB signaling pathway. Moreover, immunohistochemical staining with FATP3 and FATP4 antibodies was used to visualize FATP3 and FATP4 expression in endothelial cells in the hearts. In agreement with the quantitative reverse transcription–PCR results, a significant increase in FATP4 expression and a minor

increase of FATP3 expression were observed in $ApoE^{-/-}$/$PEDF^{-/-}$ mice (Figure 6C and 6D).

PEDF Negatively Regulates VEGFB in Peripheral Tissues in Hyperlipidemia

To further explore whether PEDF expression is relevant to FA uptake mediated by the VEGFB signaling pathway, we also determined serum VEGFB levels in patients with ASCVD and individuals without ASCVD to detect the relationship between PEDF and VEGFB. Compared with subjects without ASCVD, patients with ASDVD showed significantly higher serum VEGFB levels (0.86 [0.05–4.63] versus 1.26 [0.05–5.38] ng/mL; $P<0.05$) (Figure 7A). The data of serum VEGFB level in brackets are the range, (minimum, maximum). However, stepwise multivariate regression analysis indicated that serum VEGFB levels independently correlated with serum PEDF levels (β [95% CI], −0.711 [−1.200 to −0.223]; $P<0.01$) (Table S8), and
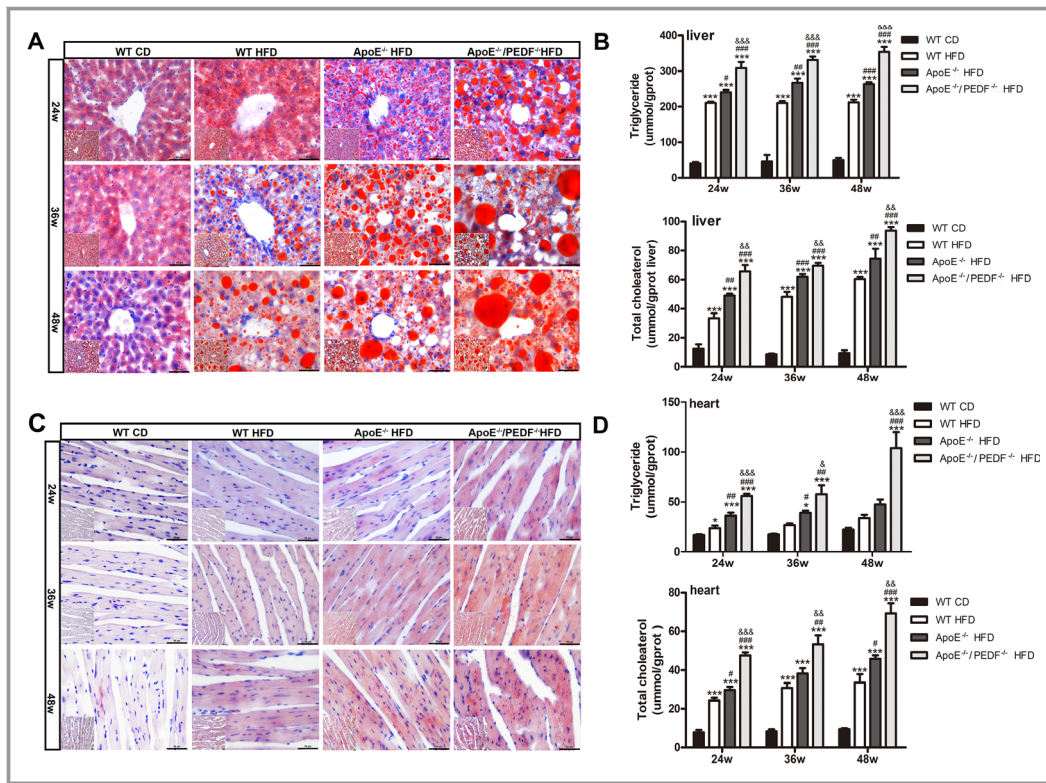
Figure 5. Pigment epithelial-derived factor deficiency (PEDF$^{-/-}$) aggravates lipid accumulation in peripheral tissues. Representative images show lipid droplets in the liver (**A**), heart (**C**), and skeletal muscle (**E**) sections from wild-type (WT) (chow diet [CD]), WT, apolipoprotein E–deficient (ApoE$^{-/-}$), and ApoE$^{-/-}$/PEDF$^{-/-}$ mice fed high-fat diet (HFD) for 24, 36, and 48 weeks by oil red O staining (per group, n=4–6); triglyceride and total cholesterol (TC) concentrations in the liver (**B**), heart (**D**), and skeletal muscle (**F**) were measured by assay kits (per group, n=5–7). **G**, Representative images show lipid droplets in the liver, heart, and skeletal muscle sections. **H**, Analysis of triglyceride and TC concentrations is shown in adeno-associated virus (AAV)–control, AAV–green fluorescent protein (GFP), and AAV-PEDF mice fed HFD for 36 weeks (per group, n=4–5) (magnification ×20 and ×40; bar=50 μm). Data are presented as mean±SE. *$P<0.05$, **$P<0.01$, ***$P<0.001$ vs WT CD; #$P<0.05$, ##$P<0.01$, ###$P<0.001$ vs WT HFD; &$P<0.05$, &&$P<0.01$, &&&$P<0.001$ vs ApoE$^{-/-}$ HFD; $\$P<0.05$, $\$\$P<0.01$, vs AAVCON HFD; +$P<0.05$,++$P<0.01$ vs AAV-GFP HFD.

Pearson's correlation analysis revealed that serum PEDF levels were negatively correlated with serum VEGFB levels ($R=-0.207$; $P<0.01$) (Figure 7B). In addition, transcriptional profiling and protein expression of VEGFB in heart, skeletal muscle, and adipose tissue were determined in ApoE$^{-/-}$/PEDF$^{-/-}$, ApoE$^{-/-}$, and WT mice after 24 weeks of HFD or CD. Quantitative reverse transcription–PCR analysis showed that VEGFB expression was significantly upregulated in the hearts and skeletal muscles from PEDF–deficient mice; the same results were found for VEGFB protein expression in the hearts from ApoE$^{-/-}$/PEDF$^{-/-}$ mice after 36 weeks of HFD by immunohistochemical staining, but VEGFB protein expression was downregulated in adipose tissues compared with that in the other groups (Figure 7E and 7F). Moreover, Western blot analysis revealed that VEGFB expression decreased in mouse aortic smooth muscle cells, C2C12 cells, and neonatal mouse cardiomyocytes treated with

increasing concentrations of human recombinant PEDF (0, 10, 25, 50, 100, and 200 nmol/L) for 24 hours or with 100 nmol/L PEDF for increasing times (0, 0.5, 3, 6, 12, and 24 hours) (Figure 7C and 7D).

PEDF Modulates Receptors of the VEGFB-Mediated Signaling Pathway in Endothelial Cells

VEGFB is bound specifically to VEGFR1 and its coreceptor NRP1 on endothelial cells to regulate FA transport. Immunostaining with a VEGFR1 or NRP1 antibody was used to visualize endothelium cells, as indicated by colocalization with the vessel-specific marker protein CD31, in the hearts of ApoE$^{-/-}$/PEDF$^{-/-}$, ApoE$^{-/-}$, and WT mice after 36 weeks of HFD or CD. An obvious upregulation of VEGFR1 expression, as well as NRP1 expression, was found in ApoE$^{-/-}$/PEDF$^{-/-}$ mice
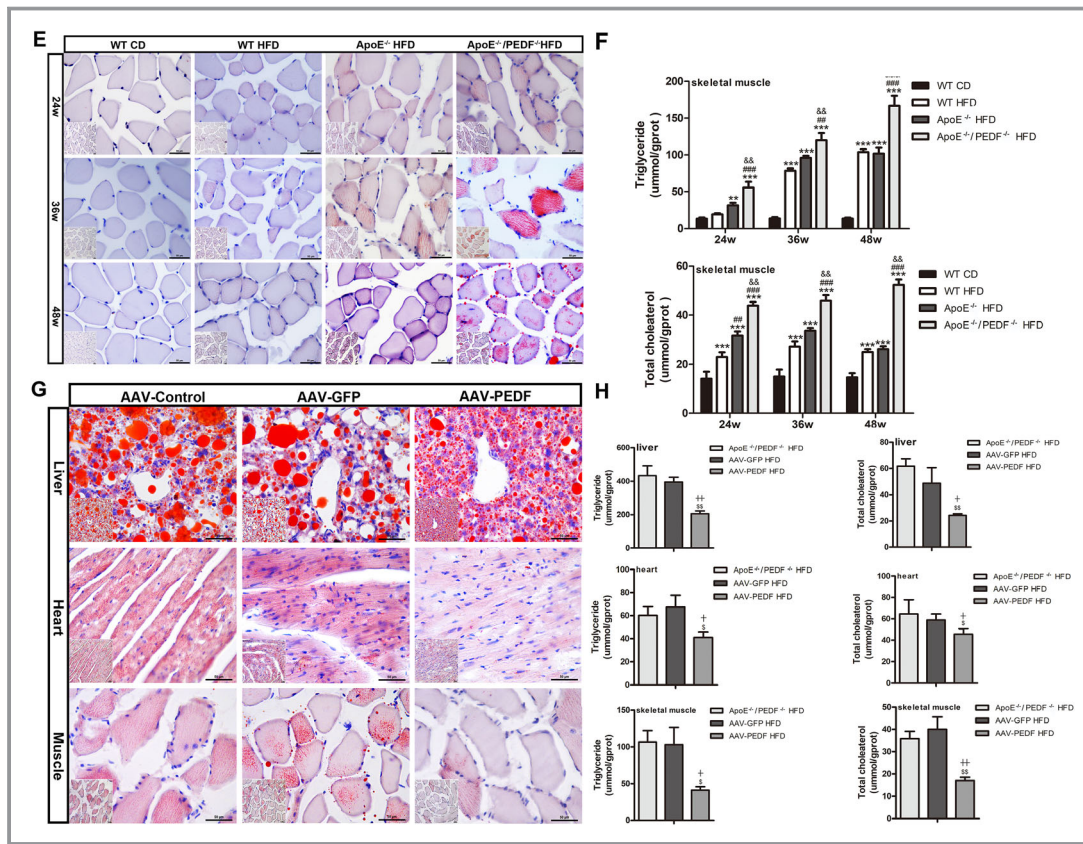
Figure 5. Continued

compared with that in other groups (Figure 8A and 8B). Furthermore, lower expression levels of VEGFR1 and NRP1 were observed in HUVECs after treatment with 100 nmol/L PEDF for 24 hours. Correspondingly, when HUVECs were exposed to 100 nmol/L PEDF in combination with 100 nmol/L human recombinant VEGFB, remarkable down-regulation of VEGFR1 and NRP1 was observed, contrary to their upregulation after the addition of 100 nmol/L VEGFB alone. When neutralizing antibodies to PEDF were added in combination with 100 nmol/L PEDF and 100 nmol/L VEGFB, the downregulation of VEGFR1 and NRP1 expression by PEDF was completely eliminated (Figure 8C and 8D). In addition, similar results were obtained by Western blot of HUVECs (Figure 8F). Moreover, we cultured HUVECs with the same treatments as above and quantified the cellular uptake of fluorescent FAs. PEDF protein treatment in HUVECs in the presence or absence of VEGFB led to a decrease in cellular FA uptake. Nevertheless, the capacity of FA uptake in cells conversely increased when polyclonal antibodies against PEDF were added (Figure 8E). In a nutshell, we concluded that PEDF could downregulate the protein expression of the VEGFB signaling pathway, including VEGFR1, NRP1, FATP3, and FATP4, to reduce endothelium-mediated FA uptake.

Discussion

In this study, we investigated the dynamic variations of circulating PEDF levels on vascular function and structure and the role of PEDF in lipid metabolism via VEGFB signaling pathway mediation of endothelial FA uptake under hyperlipidemic conditions. First, our study showed significantly higher serum PEDF levels in patients with ASCVD with dyslipidemia than in control subjects, which is consistent with previously reported metabolic syndrome data.[14,37,38] Researchers have speculated that increased serum PEDF levels may play a protective role in counteracting vascular damage by hyper-triglyceridemia, hyperglycemia, and chronic inflammation.[17,38,39] However, these studies focused on clinical research, and few animal studies of CVD were performed; this fact may have limited the further exploration of the relationship of serum PEDF levels with atherosclerosis. Because serum PEDF levels were measured in a clinical study at a single time point, it is difficult to determine the dynamic characteristics of PEDF levels in CVD. To overcome this limitation and establish definitive causal relationships between circulating PEDF levels and metabolic disorders, dynamic changes in plasma PEDF levels were determined in WT and ApoE$^{-/-}$ mice fed a long-term HFD. Serum levels of
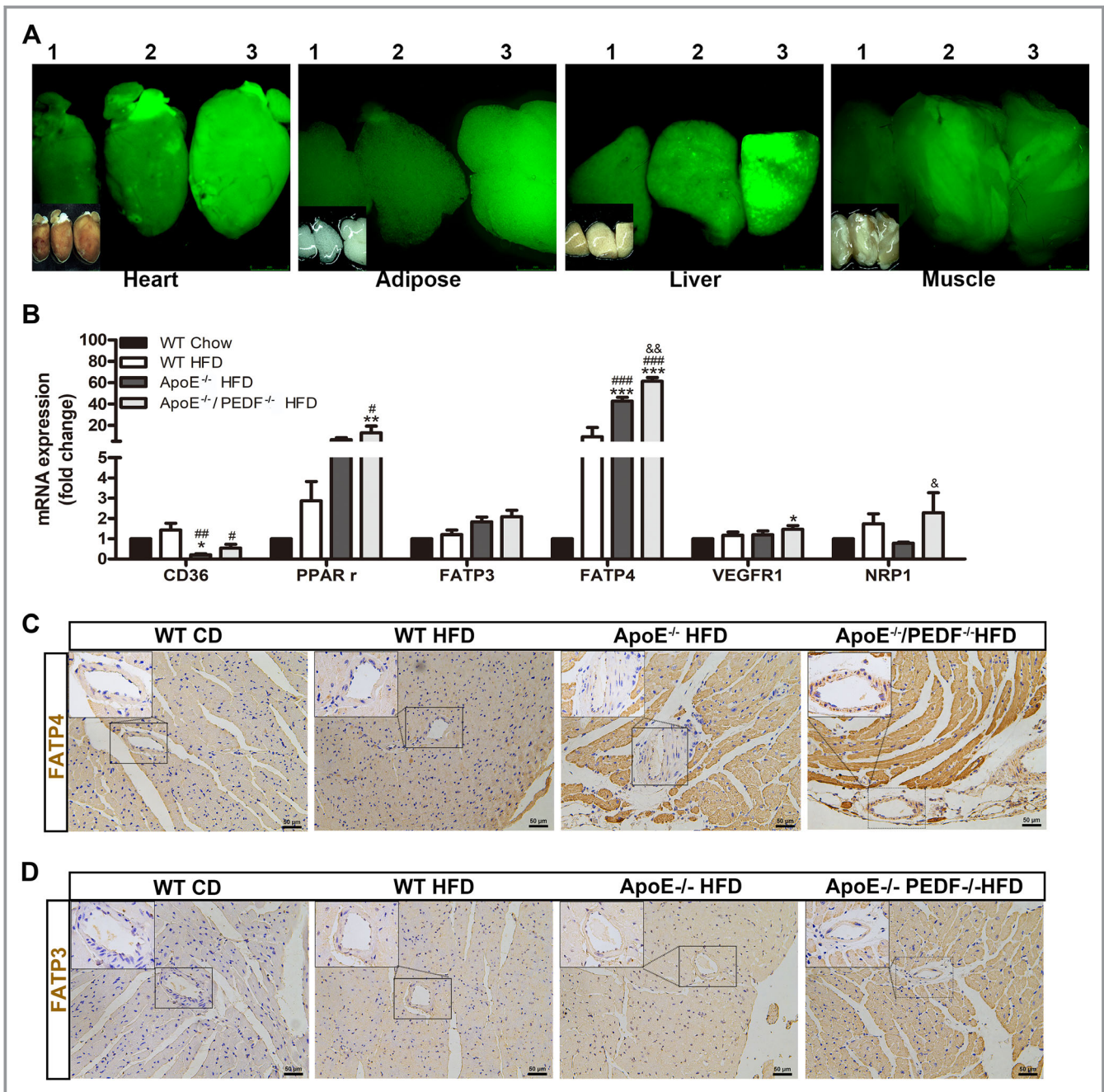
Figure 6. Vascular endothelial growth factor B signaling pathway mediating endothelial fatty acid (FA) uptake is activated in high-fat diet (HFD)–fed mice lacking pigment epithelial-derived factor (PEDF) expression. **A**, Representative images show 4,4-difluoro-3a,4adiaza-s-indacene–FA uptake in wild-type (WT), apolipoprotein E deficient (ApoE$^{-/-}$), and ApoE$^{-/-}$/PEDF-deficient (PEDF$^{-/-}$) mice fed HFD for 36 weeks (1, WT mice; 2, ApoE$^{-/-}$ mice; 3, ApoE$^{-/-}$/PEDF$^{-/-}$ mice; n=3). **B**, Relative RNA expression of endothelium-mediated FA transporter genes of FA translocase (cd36), peroxisome proliferator-activated receptor γ (ppar-γ), fatty acid transport protein 3 and 4 (fatp3/4), vascular endothelial growth factor receptor 1 (vegfr1), and neuropilin 1 (nrp1) in the hearts from WT, ApoE$^{-/-}$, and ApoE$^{-/-}$/PEDF$^{-/-}$ mice fed HFD for 24 weeks and age-matched WT mice fed chow diet (CD) (n=4–5 per genotype). **C**, Immunohistochemical localization of FATP4. **D**, FATP3 in endothelial cells in the heart sections from WT, ApoE$^{-/-}$, and ApoE$^{-/-}$/PEDF$^{-/-}$ mice fed HFD for 36 weeks and age-matched WT mice fed CD (n=3–4 per genotype) (bar=50 μm). Data are presented as mean±SE. *$P<0.05$, **$P<0.01$, ***$P<0.001$ vs WT CD; #$P<0.05$, ##$P<0.01$, ###$P<0.001$ vs WT HFD; &$P<0.05$, &&$P<0.01$ vs ApoE$^{-/-}$ HFD.

PEDF continuously increased until 12 weeks, which is in agreement with the reported clinical research. Interestingly, decreasing trends were detected in both WT and ApoE$^{-/-}$ mice with increasing HFD induction time, but there was little difference between age-matched WT and ApoE$^{-/-}$ mice on a CD. These findings suggest that circulating PEDF levels are
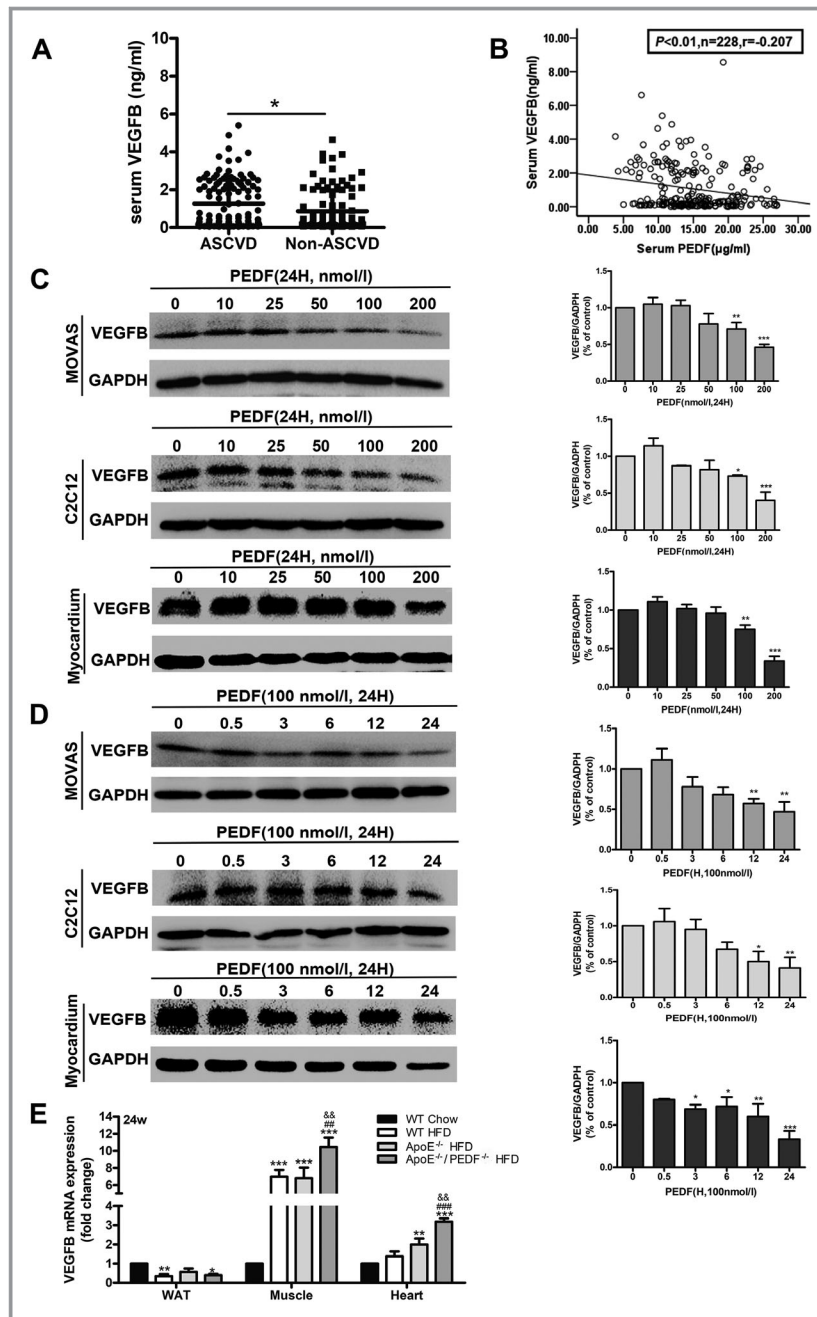
Figure 7. Vascular endothelial growth factor B (VEGFB) expression is negatively regulated by pigment epithelial-derived factor (PEDF) in peripheral tissues. **A**, Comparison of serum VEGFB levels in participants with and without atherosclerotic cardiovascular disease (ASCVD). **B**, Correlation between serum PEDF levels and serum VEGFB levels. VEGFB protein expression in mouse aortic smooth muscle cells (MOVAS), mouse myoblasts (C2C12), and neonatal mouse cardiac cells after treatments with increasing concentration of human recombinant PEDF (0, 10, 25, 50, 100 and 200 nmol/L) for 24 hours (**C**) or with 100 nmol/L PEDF for increasing time (0, 0.5, 3, 6, 12 and 24 hours) (**D**) (n=3). **E**, Relative RNA expression of vegfb in white adipose tissue, heart, and skeletal muscle in wild-type (WT), apolipoprotein E–deficient (ApoE$^{-/-}$), and ApoE$^{-/-}$/PEDF-deficient mice fed high-fat diet (HFD) for 24 weeks and age-matched WT fed chow diet (CD). **F**, Immunohistochemical localization of VEGFB in the heart sections of WT (CD), WT, ApoE$^{-/-}$, and ApoE$^{-/-}$/PEDF$^{-/-}$ mice fed HFD for 36 weeks (n=3–4 per genotype) (bar=50 μm). Data are presented as mean±SE. *$P<0.05$, **$P<0.01$, ***$P<0.001$ vs WT CD; $^{##}P<0.01$, $^{###}P<0.001$ vs WT HFD; $^{&&}P<0.01$ vs ApoE$^{-/-}$ HFD.
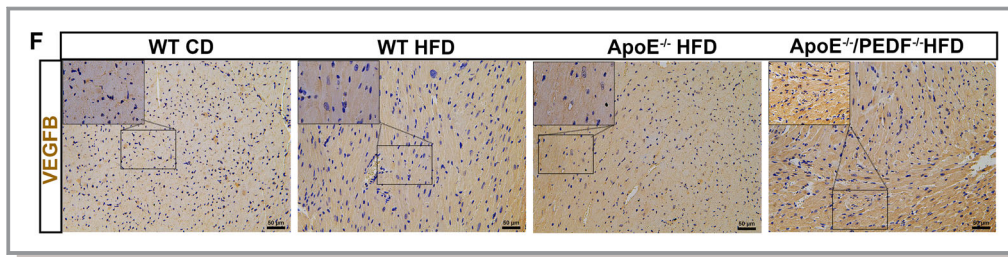
Figure 7. Continued

decreased in the later stage of atherosclerosis. Surprisingly, the serum levels of PEDF in WT mice were higher than those in ApoE$^{-/-}$ mice after 12 weeks of HFD, although there was no statistical difference between the mean values. Given the increase of serum PEDF levels observed in chow-fed ApoE$^{-/-}$ mice at 8 weeks compared with age- and sex-matched WT mice (Figure S1C), we are inclined toward the hypothesis that the early compensatory increase and the late decompensated decrease of serum PEDF levels appeared earlier in ApoE$^{-/-}$ mice than those in WT mice.

In addition, our results demonstrated that PEDF plays a protective role in the later stage of progressive atherosclerosis on the basis of the following observations. PEDF deficiency in ApoE$^{-/-}$ mice was associated with greater increases in body weight, epididymal fat pads, abdominal and subcutaneous fat, and serum lipid levels compared with those in ApoE$^{-/-}$ mice after 24, 36, and 48 weeks of HFD. In addition, PEDF-deficient mice had accelerated atherosclerotic plaque formation and aggravated lipid deposition in peripheral tissues compared with control mice. Accordingly, PEDF deficiency in ApoE$^{-/-}$ mice fed a long-term HFD had exacerbated endothelial dysfunction, as evidenced by significantly increased BP (SBP, DBP, and mean BP), markedly increased arterial stiffness (PWV and ascending aorta and descending aorta blood velocity), and observably impaired endothelial vasodilation compared with control mice; however, PEDF supplementation by AAV-PEDF injection resulted in the opposite effects. These observations further confirmed that PEDF protectively maintains vascular function in the later stages of atherosclerosis.

PEDF deletion aggravates lipid accumulation in peripheral tissues, illustrating that PEDF may regulate endothelial FA uptake. Other than the unregulated, passive diffusion of substrates across cell membranes, the membrane transport process must be regulated in a specific manner because of the selective accumulation of lipids at specific body sites in obesity.[40] On the basis of key endothelial signaling mechanisms involving VEGFB and peroxisome proliferator-activated receptor-γ in the regulation of FA transport,[6,41] transcriptional and protein analysis revealed consistent increasing trends of key genes, including FATP3, FATP4, VEGFR1, and NRP-1, in ApoE$^{-/-}$/PEDF$^{-/-}$ mice compared

with those in the other mice, revealing that PEDF could regulate the VEGFB signaling pathway to mediate endothelial FA uptake. VEGFB signaling involves modulating pathological lipid accumulation in diabetes mellitus, obesity, and CVD and is regulated by a set of nuclear-encoded mitochondrial genes that affect FA uptake.[7,42,43] More evidence suggests that PEDF could block the VEGFB signaling pathway to mediate endothelial FA uptake. First, a clinical study showed negative correlation coefficients between serum PEDF levels and serum VEGFB levels. Second, in vitro and in vivo experiments demonstrated that PEDF could downregulate VEGFB expression in peripheral tissues. Third, PEDF could suppress the expression of VEGFB-targeted receptors and FA transporters, including VEGFR1, NRP-1, FATP3, and FATP4, in HUVECs. Upregulation of VEGFR1 and NRP-1 expression was observed in ApoE$^{-/-}$/PEDF$^{-/-}$ mice, which increased endothelial FA uptake.

Altogether, as shown in the schematic diagram of the mechanism (Figure 9), we hypothesized that high serum levels of PEDF play a policing role in maintaining lipid metabolism in the normal physiological state. When metabolic disorders occur in the early stage, increased serum levels of PEDF may be a quick response to metabolic syndrome as a compensatory system to help prevent the development of obesity-induced hyperlipidemia. However, in the late stage of hyperlipidemia, decreased serum PEDF levels may have a decompensatory role in which the defensive function against atherosclerosis is lost. The negative regulation of PEDF on VEGFB signaling may become uncontrollable, which thus activates the VEGFB signaling pathway. Upregulation of VEGFB in tissue cells, its receptors VEGFR1 and NRP1, and FA transporters FATP3/4 in endothelial cells accelerate FA uptake, causing lipid accumulation in peripheral tissues.

The VEGF family, comprising VEGFA, VEGFB, VEGFC, and placental growth factor, signals via the endothelial receptors VEGFR1 and VEGFR2; and its members are major regulators of blood vessel physiological characteristics.[44] Although numerous studies have shown that PEDF effectively abates VEGF-induced angiogenesis and vascular permeability, especially VEGFA, there are few studies on the relation between PEDF and VEGFB. In addition, PEDF is also able to regulate the
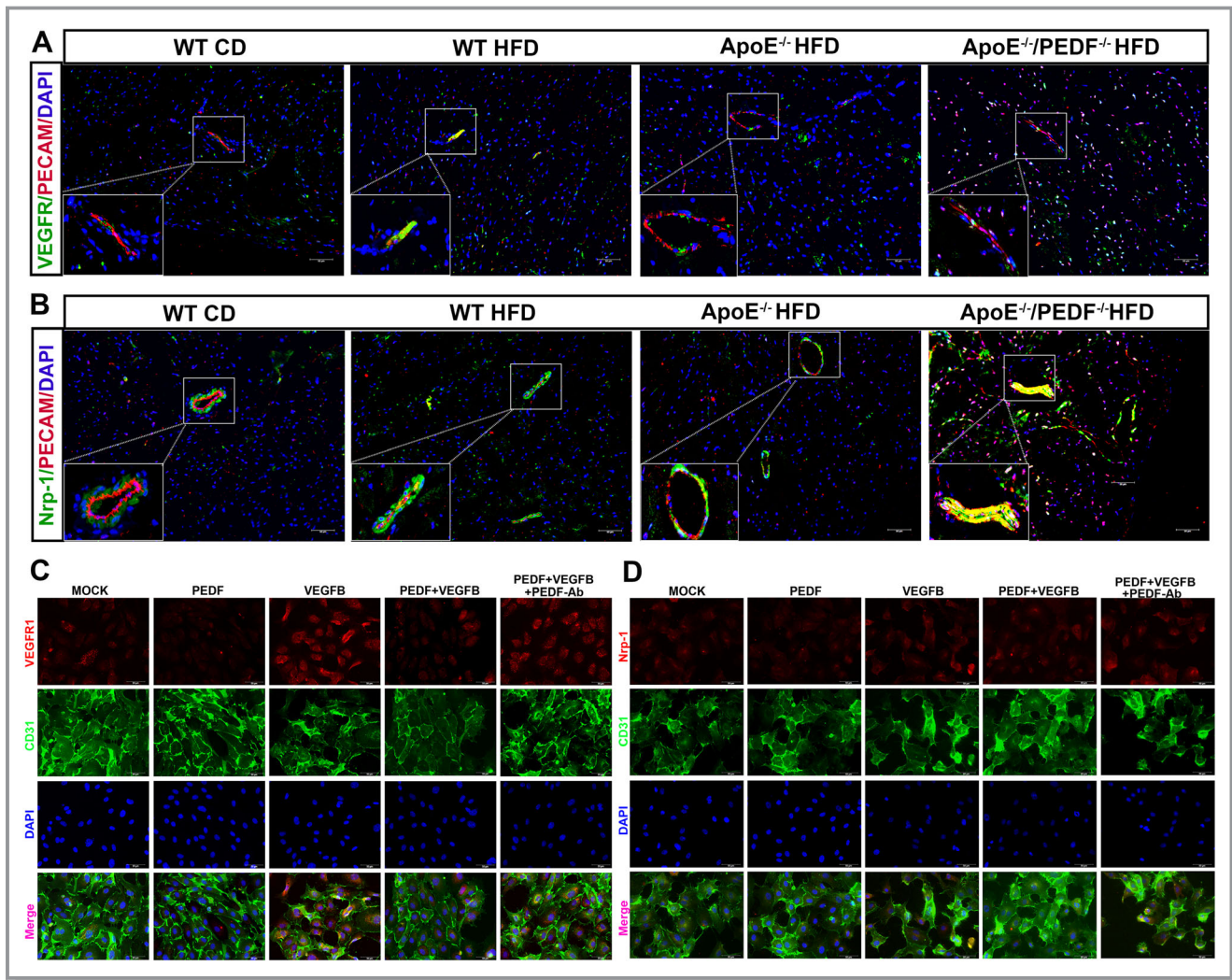
Figure 8. Pigment epithelial–derived factor (PEDF) inhibits expression of vascular endothelial growth factor B (VEGFB)–targeted receptors in endothelial cells. Representative images of heart sections visualized with anti–vascular endothelial growth factor receptor 1 (VEGFR1) (**A**) or anti–neuropilin 1 (NRP1) (**B**) antibody and colocalized with CD31 (endothelial marker) antibody from wild-type (WT), apolipoprotein E–deficient (ApoE$^{-/-}$), and ApoE$^{-/-}$/PEDF-deficient (PEDF$^{-/-}$) mice fed high-fat diet (HFD) for 36 weeks and age–matched WT fed chow diet (CD) (n=3–4 per genotype). Merged images appear as yellow. **C**, Representative immunofluorescent images of human umbilical vein endothelial cells (HUVECs) treated with mock (unstimulated), 100 nmol/L PEDF alone, 100 ng/mL VEGFB alone, 100 ng/mL VEGFB+100 nmol/L PEDF, and 100 ng/mL VEGFB+100 nmol/L PEDF+PEDF neutralizing antibody (PEDF-Ab) for 24 hours. **D**, Cultures were triple stained for VEGFR1 (red) or NRP1 (red) with CD31 (green) (magnification ×20; bar=50 μm). **E**, Protein expression of VEGFR1, NRP1, fatty acid transport protein (FATP) 3, and FATP4 in HUVECs after treatments with mock, increasing concentrations of VEGFB (25, 50, and 100 ng/mL), 100 ng/mL VEGFB+100 nmol/L PEDF, and 100 ng/mL VEGFB+100 nmol/L PEDF+PEDF-Ab for 24 hours (n=4). **F**, 4,4-Difluoro-3a,4adiaza-s-indacene—fatty acid uptake into HUVECs after the same treatments as above (n=3). Data are presented as mean±SE. DAPI indicates 4′,6-diamidino-2-phenylindole; PECAM, platelet endothelial cell adhesion molecule 1. *P<0.05, ***P<0.001.

phosphorylation of VEGFR1 as well as enhance γ-secretase–dependent cleavage of the C terminus of VEGFR1 to inhibit VEGFA-induced angiogenesis.[45,46] Nevertheless, in addition to the target molecules in the VEGFB-VEGFR1/NRP1-FATP3/4 signaling pathway, whether there are other target molecules involved in endothelium–mediated FA transport and the role of PEDF in this pathway need to be further studied and discussed.

We did not analyze the sex-based differences in clinical cardiovascular research. Furthermore, in vivo animal-based studies, only male mice were used. It may limit the generalizability of our findings, although several studies have observed the similar trend of changes between male and female subjects in CVD.[37,47] Another limitation of this study is that we have not explained the reason why similar serum levels of PEDF in WT and ApoE$^{-/-}$ mice on HFD resulted in
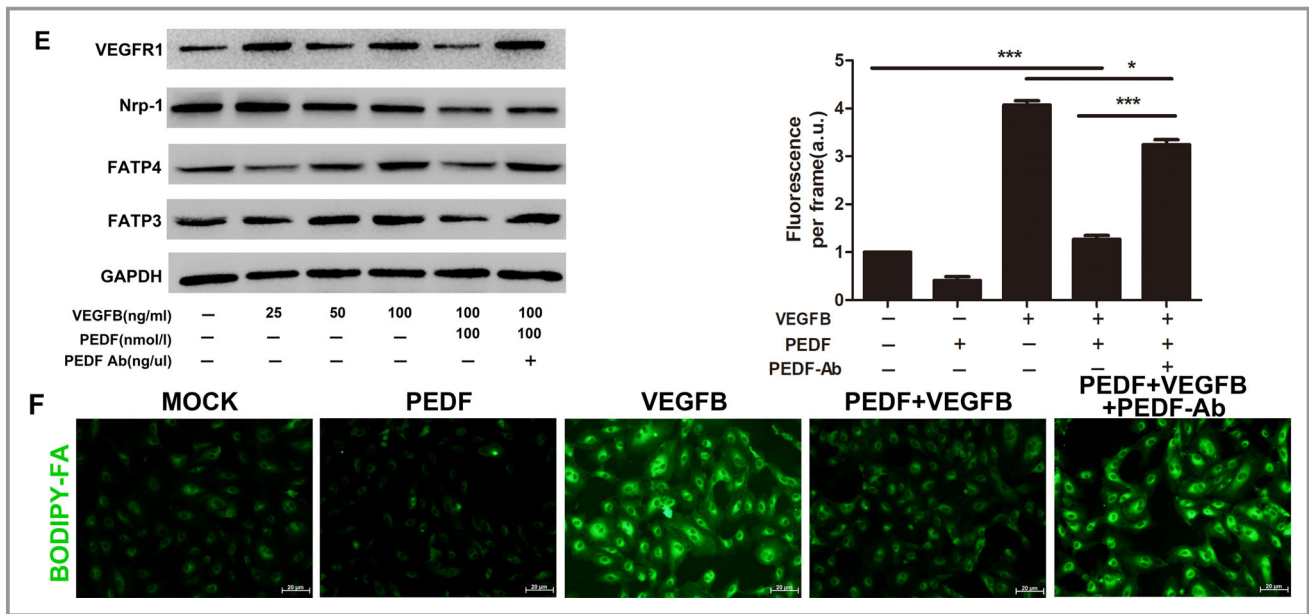
Figure 8. Continued

significant differences in epididymal fat pad weight, visceral and subcutaneous fat, and the extent of atherosclerotic lesions. Considering that lipid metabolism is likely to be regulated by a variety of complex mechanisms, we speculated that there are differences in lipid metabolism between WT and ApoE$^{-/-}$ mice. In addition, researchers suggested that elevated serum PEDF level might be a response to counteract the generation of the proatherosclerotic environment caused by vascular damage in early metabolic syndrome. However, in

our current study, the exact mechanism of the decrease of serum PEDF level in late stage of atherosclerosis has not been solved; and more studies are needed.

In conclusion, the current study highlighted that PEDF exerts beneficial effects on atherosclerotic lesions, vascular function and structure, and lipid homeostasis by regulating the VEGFB-VEGFR1/NRP1-FATP3/4 signaling pathway to mediate endothelial FA uptake in hyperlipidemia. These novel findings are relevant to enhancing our
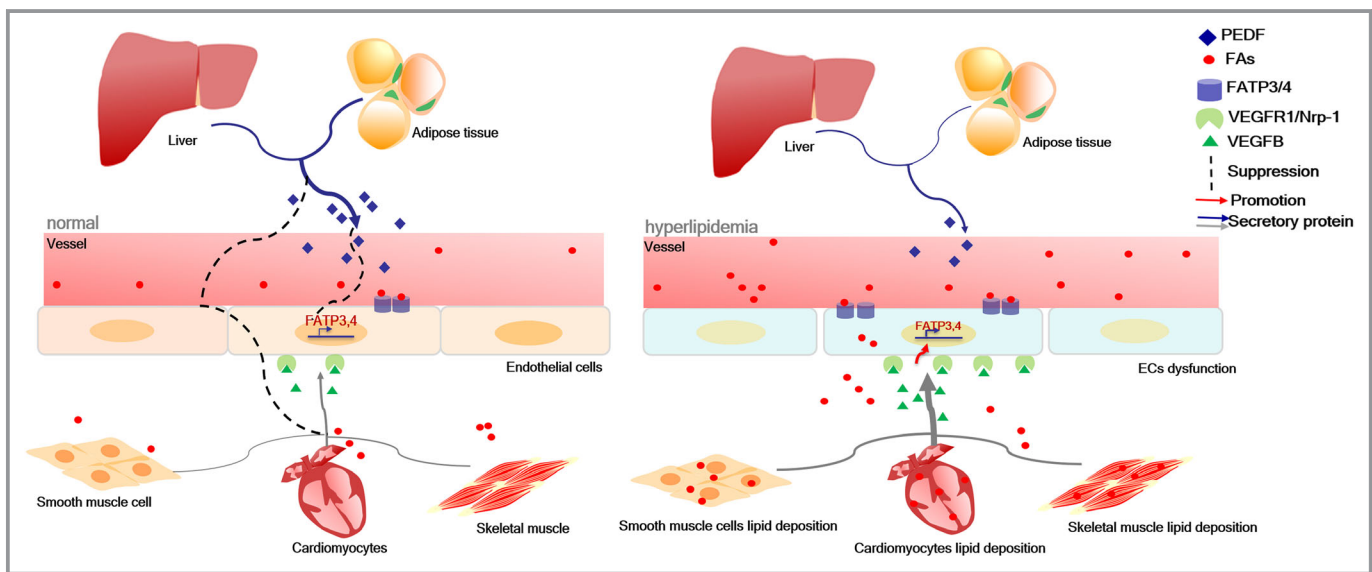
Figure 9. Schematic diagram of the mechanisms of pigment epithelial-derived factor (PEDF) regulation on vascular endothelial growth factor B (VEGFB) signaling affect endothelium-mediated fatty acid (FA) uptake in normal state and in condition of hyperlipidemia. EC indicates endothelial cell; FATP3/4, FA transport proteins 3 and 4; VEGFR1/Nrp-1, vascular endothelial growth factor receptor 1 and the coreceptor neuropilin 1.

understanding of the pathogenesis of atherosclerosis and indicate that PEDF and VEGFB-VEGFR1/NRP1-FATP3/4 could act as novel potential therapeutic targets in atherosclerosis.

Acknowledgments

Sources of Funding

Disclosures

None.

References

1. Gimbrone MA Jr, Garcia-Cardena G. Endothelial cell dysfunction and the pathobiology of atherosclerosis. *Circ Res*. 2016;118:620–636.

2. Shapiro MD, Fazio S. From lipids to inflammation: new approaches to reducing atherosclerotic risk. *Circ Res*. 2016;118:732–749.

3. Ridker PM. Hyperlipidemia as an instigator of inflammation: inaugurating new approaches to vascular prevention. *J Am Heart Assoc*. 2012;1:e000497. DOI: 10.1161/JAHA.112.000497.

4. Pi X, Xie L, Patterson C. Emerging roles of vascular endothelium in metabolic homeostasis. *Circ Res*. 2018;123:477–494.

5. Rodriguez-Lee M, Bondjers G, Camejo G. Fatty acid-induced atherogenic changes in extracellular matrix proteoglycans. *Curr Opin Lipidol*. 2007;18:546–553.

6. Mehrotra D, Wu J, Papangeli I, Chun HJ. Endothelium as a gatekeeper of fatty acid transport. *Trends Endocrinol Metab*. 2014;25:99–106.

7. Hagberg CE, Falkevall A, Wang X, Larsson E, Huusko J, Nilsson I, van Meeteren LA, Samen E, Lu L, Vanwildemeersch M, Klar J, Genove G, Pietras K, Stone-Elander S, Claesson-Welsh L, Yla-Herttuala S, Lindahl P, Eriksson U. Vascular endothelial growth factor B controls endothelial fatty acid uptake. *Nature*. 2010;464:917–921.

8. Hagberg C, Mehlem A, Falkevall A, Muhl L, Eriksson U. Endothelial fatty acid transport: role of vascular endothelial growth factor B. *Physiology (Bethesda)*. 2013;28:125–134.

9. Muhl L, Moessinger C, Adzemovic MZ, Dijkstra MH, Nilsson I, Zeitelhofer M, Hagberg CE, Huusko J, Falkevall A, Yla-Herttuala S, Eriksson U. Expression of vascular endothelial growth factor (VEGF)-B and its receptor (VEGFR1) in murine heart, lung and kidney. *Cell Tissue Res*. 2016;365:51–63.

10. Dai Z, Qi W, Li C, Lu J, Mao Y, Yao Y, Li L, Zhang T, Hong H, Li S, Zhou T, Yang Z, Yang X, Gao G, Cai W. Dual regulation of adipose triglyceride lipase by pigment epithelium-derived factor: a novel mechanistic insight into progressive obesity. *Mol Cell Endocrinol*. 2013;377:123–134.

11. Lu P, Zhang YQ, Zhang H, Li YF, Wang XY, Xu H, Liu ZW, Li L, Dong HY, Zhang ZM. Pigment epithelium-derived factor (PEDF) improves ischemic cardiac functional reserve through decreasing hypoxic cardiomyocyte contractility through PEDF receptor (PEDF-R). *J Am Heart Assoc*. 2016;5:e003179. DOI: 10.1161/JAHA.115.003179.

12. Famulla S, Lamers D, Hartwig S, Passlack W, Horrighs A, Cramer A, Lehr S, Sell H, Eckel J. Pigment epithelium-derived factor (PEDF) is one of the most abundant proteins secreted by human adipocytes and induces insulin resistance and inflammatory signaling in muscle and fat cells. *Int J Obes (Lond)*. 2011;35:762–772.

13. Moreno-Navarrete JM, Touskova V, Sabater M, Mraz M, Drapalova J, Ortega F, Serrano N, Catalan V, Gomez-Ambrosi J, Ortiz MR, Pardo G, Pueyo N, Ricart W, Lacinova Z, Haluzik M, Fruhbeck G, Fernandez-Real JM. Liver, but not adipose tissue PEDF gene expression is associated with insulin resistance. *Int J Obes (Lond)*. 2013;37:1230–1237.

14. Gattu AK, Birkenfeld AL, Jornayvaz F, Dziura J, Li F, Crawford SE, Chu X, Still CD, Gerhard GS, Chung C, Samuel V. Insulin resistance is associated with elevated serum pigment epithelium-derived factor (PEDF) levels in morbidly obese patients. *Acta Diabetol*. 2012;49(suppl 1):S161–S169.

15. Tahara N, Yamagishi S, Kodama N, Tahara A, Honda A, Nitta Y, Igata S, Matsui T, Takeuchi M, Kaida H, Kurata S, Abe T, Fukumoto Y. Clinical and biochemical factors associated with area and metabolic activity in the visceral and subcutaneous adipose tissues by FDG-PET/CT. *J Clin Endocrinol Metab*. 2015;100:E739–E747.

16. Yamagishi S, Matsui T. Pigment epithelium-derived factor (PEDF) and cardiometabolic disorders. *Curr Pharm Des*. 2014;20:2377–2386.

17. Rychli K, Huber K, Wojta J. Pigment epithelium-derived factor (PEDF) as a therapeutic target in cardiovascular disease. *Expert Opin Ther Targets*. 2009;13:1295–1302.

18. Choi KM, Hwang SY, Hong HC, Yang SJ, Choi HY, Yoo HJ, Lee KW, Nam MS, Park YS, Woo JT, Kim YS, Choi DS, Youn BS, Baik SH. C1q/TNF-related protein-3 (CTRP-3) and pigment epithelium-derived factor (PEDF) concentrations in patients with type 2 diabetes and metabolic syndrome. *Diabetes*. 2012;61:2932–2936.

19. He J, Pham TL, Kakazu A, Bazan HEP. Recovery of corneal sensitivity and increase in nerve density and wound healing in diabetic mice after PEDF plus DHA treatment. *Diabetes*. 2017;66:2511–2520.

20. Wen H, Liu M, Liu Z, Yang X, Liu X, Ni M, Dong M, Luan X, Yuan Y, Xu X, Lu H. PEDF improves atherosclerotic plaque stability by inhibiting macrophage inflammation response. *Int J Cardiol*. 2017;235:37–41.

21. Zhang H, Sun T, Jiang X, Yu H, Wang M, Wei T, Cui H, Zhuang W, Liu Z, Zhang Z, Dong H. PEDF and PEDF-derived peptide 44mer stimulate cardiac triglyceride degradation via ATGL. *J Transl Med*. 2015;13:68.

22. Cheng G, Zhong M, Kawaguchi R, Kassai M, Al-Ubaidi M, Deng J, Ter-Stepanian M, Sun H. Identification of PLXDC1 and PLXDC2 as the transmembrane receptors for the multifunctional factor PEDF. *Elife*. 2014;3:e05401.

23. Chung C, Doll JA, Gattu AK, Shugrue C, Cornwell M, Fitchev P, Crawford SE. Anti-angiogenic pigment epithelium-derived factor regulates hepatocyte triglyceride content through adipose triglyceride lipase (ATGL). *J Hepatol*. 2008;48:471–478.

24. Borg ML, Andrews ZB, Duh EJ, Zechner R, Meikle PJ, Watt MJ. Pigment epithelium-derived factor regulates lipid metabolism via adipose triglyceride lipase. *Diabetes*. 2011;60:1458–1466.

25. Grippo PJ, Fitchev PS, Bentrem DJ, Melstrom LG, Dangi-Garimella S, Krantz SB, Heiferman MJ, Chung C, Adrian K, Cornwell ML, Flesche JB, Rao SM, Talamonti MS, Munshi HG, Crawford SE. Concurrent PEDF deficiency and Kras mutation induce invasive pancreatic cancer and adipose-rich stroma in mice. *Gut*. 2012;61:1454–1464.

26. Chung C, Shugrue C, Nagar A, Doll JA, Cornwell M, Gattu A, Kolodecik T, Pandol SJ, Gorelick F. Ethanol exposure depletes hepatic pigment epithelium-derived factor, a novel lipid regulator. *Gastroenterology*. 2009;136:331–340.e332.

27. Ma S, Yao S, Tian H, Jiao P, Yang N, Zhu P, Qin S. Pigment epithelium-derived factor alleviates endothelial injury by inhibiting Wnt/beta-catenin pathway. *Lipids Health Dis*. 2017;16:31.

28. Cai J, Wu L, Qi X, Li Calzi S, Caballero S, Shaw L, Ruan Q, Grant MB, Boulton ME. PEDF regulates vascular permeability by a gamma-secretase-mediated pathway. *PLoS One*. 2011;6:e21164.

29. Zhang H, Wang Z, Feng SJ, Xu L, Shi HX, Chen LL, Yuan GD, Yan W, Zhuang W, Zhang YQ, Zhang ZM, Dong HY. PEDF improves cardiac function in rats with acute myocardial infarction via inhibiting vascular permeability and cardiomyocyte apoptosis. *Int J Mol Sci*. 2015;16:5618–5634.

30. Hu DY, Ding RJ. Guidelines for management of adult dyslipidemia in China. *Zhonghua Nei Ke Za Zhi*. 2008;47:723–724.

31. An SM, Seong KY, Yim SG, Hwang YJ, Bae SH, Yang SY, An BS. Intracutaneous delivery of gelatins induces lipolysis and suppresses lipogenesis of adipocytes. *Acta Biomater*. 2018;67:238–247.

32. Gomez D, Baylis RA, Durgin BG, Newman AAC. Interleukin-1beta has atheroprotective effects in advanced atherosclerotic lesions of mice. *Nat Med*. 2018;24:1418–1429.

33. Singh MV, Kotla S, Le NT, Ae Ko K, Heo KS, Wang Y, Fujii Y, Thi VᴜH, McBeath E, Thomas TN, Jin Gi Y, Tao Y, Medina JL, Taunton J, Carson N, Dogra V, Doyley MM, Tyrell A, Lu W, Qiu X, Stirpe NE, Gates KJ, Hurley C, Fujiwara K, Maggirwar SB, Schifitto G, Abe JI. Senescent phenotype induced by p90RSK-NRF2 signaling sensitizes monocytes and macrophages to oxidative stress in HIV-positive individuals. *Circulation*. 2019;139:1199–1216.

34. Khalifeh-Soltani A, McKleroy W, Sakuma S, Cheung YY, Tharp K, Qiu Y, Turner SM, Chawla A, Stahl A, Atabai K. Mfge8 promotes obesity by mediating the uptake of dietary fats and serum fatty acids. *Nat Med*. 2014;20:175–183.

35. Crowe S, Wu LE, Economou C, Turpin SM, Matzaris M, Hoehn KL, Hevener AL, James DE, Duh EJ, Watt MJ. Pigment epithelium-derived factor contributes to insulin resistance in obesity. *Cell Metab*. 2009;10:40–47.

36. Balakumar P, Kathuria S. Submaximal ppargamma activation and endothelial dysfunction: new perspectives for the management of cardiovascular disorders. *Br J Pharmacol*. 2012;166:1981–1992.

37. Chen C, Tso AW, Law LS, Cheung BM, Ong KL, Wat NM, Janus ED, Xu A, Lam KS. Plasma level of pigment epithelium-derived factor is independently associated with the development of the metabolic syndrome in Chinese men: a 10-year prospective study. *J Clin Endocrinol Metab*. 2010;95:5074–5081.

38. Wang F, Ma X, Zhou M, Pan X, Ni J, Gao M, Lu Z, Hang J, Bao Y, Jia W. Serum pigment epithelium-derived factor levels are independently correlated with the presence of coronary artery disease. *Cardiovasc Diabetol*. 2013;12:56.

39. Yamagishi S, Matsui T, Nakamura K. Atheroprotective properties of pigment epithelium-derived factor (PEDF) in cardiometabolic disorders. *Curr Pharm Des*. 2009;15:1027–1033.

40. Berk PD. Regulatable fatty acid transport mechanisms are central to the pathophysiology of obesity, fatty liver, and metabolic syndrome. *Hepatology*. 2008;48:1362–1376.

41. Goto K, Iso T, Hanaoka H, Yamaguchi A, Suga T, Hattori A, Irie Y, Shinagawa Y, Matsui H, Syamsunarno MR, Matsui M, Haque A, Arai M, Kunimoto F, Yokoyama T, Endo K, Gonzalez FJ, Kurabayashi M. Peroxisome proliferator-activated receptor-gamma in capillary endothelia promotes fatty acid uptake by heart during long-term fasting. *J Am Heart Assoc*. 2013;2:e004861. DOI: 10.1161/JAHA.112.004861.

42. Karpanen T, Bry M, Ollila HM, Seppanen-Laakso T, Liimatta E, Leskinen H, Kivela R, Helkamaa T, Merentie M, Jeltsch M, Paavonen K, Andersson LC, Mervaala E, Hassinen IE, Yla-Herttuala S, Oresic M, Alitalo K. Overexpression of vascular endothelial growth factor-B in mouse heart alters cardiac lipid metabolism and induces myocardial hypertrophy. *Circ Res*. 2008;103:1018–1026.

43. Mehlem A, Palombo I, Wang X, Hagberg CE, Eriksson U, Falkevall A. PGC-1a coordinates mitochondrial respiratory capacity and muscular fatty acid uptake via regulation of VEGF-B. *Diabetes*. 2016;65:861–873.

44. Tammela T, Enholm B, Alitalo K, Paavonen K. The biology of vascular endothelial growth factors. *Cardiovasc Res*. 2005;65:550–563.

45. Cai J, Jiang WG, Grant MB, Boulton M. Pigment epithelium-derived factor inhibits angiogenesis via regulated intracellular proteolysis of vascular endothelial growth factor receptor 1. *J Biol Chem*. 2006;281:3604–3613.

46. Cai J, Chen Z, Ruan Q, Han S, Liu L, Qi X, Boye SL, Hauswirth WW, Grant MB, Boulton ME. Gamma-secretase and presenilin mediate cleavage and phosphorylation of vascular endothelial growth factor receptor-1. *J Biol Chem*. 2011;286:42514–42523.

47. Marz W, Scharnagl H, Winkler K, Tiran A, Nauck M, Boehm BO, Winkelmann BR. Low-density lipoprotein triglycerides associated with low-grade systemic inflammation, adhesion molecules, and angiographic coronary artery disease: the Ludwigshafen Risk and Cardiovascular Health Study. *Circulation*. 2004;110:3068–3074.

Supplemental Material

Table S1. PCR primer sequences. All sequences are written 5'-3'.

Genes	Primer sequences
ApoE gene	Primer 1 common:5'-GCCTAGCCGAGGGAGAGCCG-3'
	Primer 2 WT R :5'-TGTGACTTGGGAGCTCTGCAGC-3'
	Primer 3 Mut R :5'-GCCGCCCCGACTGCATCT-3'
PEDF gene	Primer A 163 SU :5'-AAGACCTCAAGTCAAGGGTC-3'
	Primer B 163 SD :5'-CATAAGGACCAGTTTCTCTCC-3'
	Primer C PGK :5'-TCATTCTCAGTATTGTTTTGCC-3'
	Primer D 163 TUR:5'-CTGCCTCCCTGCACTGTCTC-3'

Table S2. Enzymatic kits for plasma measurements.

Types of enzymatic kit	Source	Catalog #
Triglyceride	Nanjing Jiancheng Bioengineering Institute (Nanjing, China)	A110-1
Total cholesterol	Nanjing Jiancheng Bioengineering Institute	A111-1
Low-density lipoprotein cholesterol	Nanjing Jiancheng Bioengineering Institute	A113-1
High-density lipoprotein cholesterol	Nanjing Jiancheng Bioengineering Institute	A112-1
Non-esterified fatty acids	Nanjing Jiancheng Bioengineering Institute	A042-2

Table S3. QPCR Primer sequences. All sequences are written 5'-3'.

Genes	Forward primer	Reverse primer
CD36	GATGAGCATAGGACATACTTAGATGTG	CACCACTCCAATCCCAAGTAAG
PPAR γ	CCATTCTGGCCCACCAAC	AATGCGAGTGGTCTTCCATCA
Fatp3	CGCAGGCTCTGAACCTGG	TCGAAGGTCTCCAGACAGGAG
Fatp4	GCAAGTCCCATCAGCAACTG	GGGGGAAATCACAGCTTCTC
Vegfr1	GGGGGAAATCACAGCTTCTC	TTGAGGAGCTTTCACCGAAC
Nrp-1	CGCTACCAGAAGCCAGAGGA	CATCCACAGCAATCCCACCAA
Vegfb	TCTGAGCATGGAACTCATGG	TCTGCATTCACATTGGCTGT
gapdh	TGCGACTTCAACAGCAACTC	GCCTCTCTTGCTCAGTGTCC
actin	TGACGTGGACATCCGCAAAG	CTGGAAGGTGGACAGCGAGG

Table S4. Comparison of serum biological changes in four groups of mice with 24 weeks HFD.

	24w			
	WT CD	WT HFD	ApoE$^{-/-}$ HFD	A$^{-/-}$/ P$^{-/-}$ HFD
TG (mmol/l)	0.46±0.12	0.93±0.06 (**)	1.70±0.23 (***) (###)	2.22±0.25 (***) (###) (§§)
TC (mmol/l)	2.99±0.41	4.92±0.54	14.94±2.6 (***) (###)	19.58±2.44 (***) (###) (§§)
FFA (mmol/l)	0.58±0.25	0.64±0.1	0.81±0.12	0.94±0.41 (*)
Glu (mmol/l)	6.08±0.46	7.5±0.18 (*)	8.7±0.36 (***) (#)	9.06±1.44 (***) (#)
LDL-C (mmol/l)	1.70±0.15	2.95±0.59 (**)	7.95±0.37(***) (###)	8.32±0.8 (***) (###)
HDL-C (mmol/l)	1.22±0.18	1.08±0.26	0.71±0.45 (*) (#)	0.45±0.08 (**) (##)

Table S5. Comparison of serum biological changes in four groups of mice with 36 weeks HFD.

	36w			
	WT CD	WT HFD	ApoE$^{-/-}$ HFD	A$^{-/-}$/ P$^{-/-}$ HFD
TG (mmol/l)	0.38±0.14	1.16±0.09 (*)	2.07±0.58 (***) (#)	2.95±0.46 (***) (###) (§)
TC (mmol/l)	3.2±0.59	5.97±1.01(**)	17.39±1.9 (***) (###)	23.3±1.89 (***) (###) (§§§)
FFA (mmol/l)	0.65±0.39	1.09±0.51	1.61±0.15 (**) (#)	1.78±0.38 (***) (#)
Glu (mmol/l)	6.7±0.61	7.95±0.67(*)	8.57±0.95 (**)	9.42±1.16 (***) (#)
LDL-C (mmol/l)	1.58±0.5	3.92±0.69 (*)	9.21±0.94 (***) (###)	11.69±2.1 (***) (###) (§§)
HDL-C (mmol/l)	1.11±0.28	1.03±0.22	0.38±0.24 (**) (#)	0.53±0.38 (*) (#)

Table S6. Comparison of serum biological changes in four groups of mice with 48 weeks HFD.

	48w			
	WT CD	WT HFD	ApoE$^{-/-}$ HFD	A$^{-/-}$/ P$^{-/-}$ HFD
TG (mmol/l)	0.46±0.1	1.32±0.09 (*)	2.35±0.34 (***) (#)	4.37±1.1 (***) (###) (§§§)
TC (mmol/l)	2.45±0.66	7.59±0.9 (*)	21.53±2.27(***) (###)	24.17±5.81(***) (###)
FFA (mmol/l)	0.69±0.16	1.56±0.24 (***)	1.71±0.48 (***)	1.66±0.39 (***)
Glu (mmol/l)	6.86±0.53	8.03±0.56 (*)	8.88±0.51(***)	9.55±1.28 (***) (##)
LDL-C (mmol/l)	1.27±0.41	4.27±0.52 (**)	9.8±1.1(***) (###)	12.0±2.35 (***) (###) (§)
HDL-C (mmol/l)	1.12±0.27	0.82±0.09 (**)	0.3±0.05 (***) (###)	0.32±0.06 (***) (###)

Data are expressed as mean ± SD (n=5~7 per group). TG, Triglycerides; TC, Total cholesterol; FFA, Free fatty acids; Glu, Glucose; LDL-C; LDL-cholesterol; HDL-C, HDL-cholesterol; A$^{-/-}$/P$^{-/-}$, ApoE$^{-/-}$/PEDF$^{-/-}$; CD, chow diet; HFD, high-fat diet; w, weeks. *P<0.05, **P<0.01, ***P<0.001 vs WT CD; #P<0.05, ##P<0.01, ###P<0.001 vs WT HFD; §P<0.05, §§P<0.01, §§§P<0.001 vs ApoE$^{-/-}$ HFD.

Table S7. Comparison of serum biological changes between AAV-PEDF injected mice and controls mice.

	36w HFD		
	AAV-CON	AAV-GFP	AAV-PEDF
TG (mmol/l)	2.26±0.33	2.3±0.58	1.26±0.32 (††) (‡‡)
TC (mmol/l)	19.74±2.8	21.77±4.59	11.79±1.98 (†††) (‡‡‡)
FFA (mmol/l)	1.12±0.17	1.18±0.12	0.98±0.24 (†††) (‡‡‡)
Glu (mmol/l)	9.08±0.70	8.73±0.38	8.26±0.67
LDL-C (mmol/l)	10.64±1.13	12.42±2.65	6.92±1.08 (††) (‡‡‡)
HDL-C (mmol/l)	0.31±0.19	0.32±0.06	0.96±0.24 (†††) (‡‡‡)

Data are expressed as mean ± SD (n=5~7 per group). HFD, high-fat diet; w, weeks; TG, Triglycerides; TC, Total cholesterol; FFA, Free fatty acids; Glu, Glucose; LDL-C; LDL-cholesterol; HDL-C, HDL-cholesterol; AAV-CON, ApoE$^{-/-}$/PEDF$^{-/-}$ control mice; AAV-GFP, ApoE$^{-/-}$/PEDF$^{-/-}$ mice injected AAV-GFP; AAV-PEDF, ApoE$^{-/-}$/PEDF$^{-/-}$ mice injected AAV-PEDF. $^{††}P<0.01$, $^{†††}P<0.001$ vs AAV-CON HFD, $^{‡‡}P<0.01$, $^{‡‡‡}P<0.001$ vs AAV-GFP HFD.

Table S8. Stepwise multivariate regression analysis of serum PEDF levels.

Independent variable	β	S.E.	95% CI	Standardized β	*P*
Triglyceride	0.643	0.322	(0.013,1.274)	0.150	0.0469
VEGFB	-0.711	0.248	(-1.200, -0.223)	-0.187	0.0045

Variables of the original model included: SBP, DBP, TC, TG, LDL-C, HDL-C, FFA and VEGFB.

Figure S1. Generation and analysis of DKO mice.
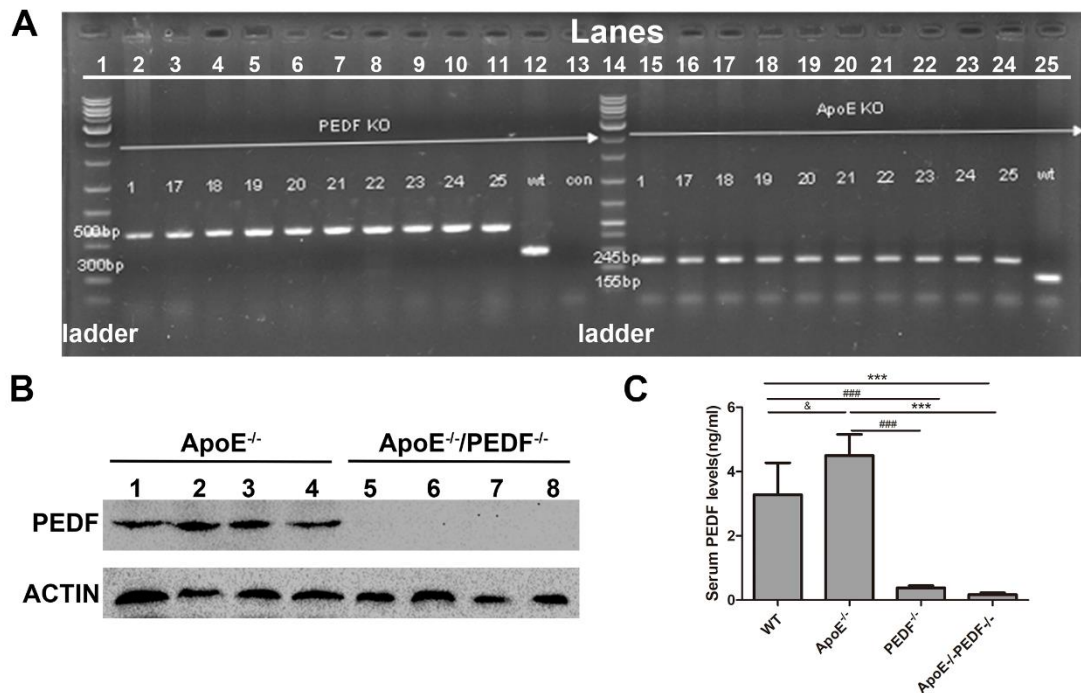
(A) The genotypes of mice used in the study were confirmed by PCR. Lanes 1, 14: Ladder: DNA molecular size marker. Lanes 2~11: Presence of band (500bp) indicates PEDF $^{(-/-)}$. Lanes 12: Presence of band (350bp) indicates PEDF $^{(+/+)}$ (from WT mice as control). Lanes 13: Blank as control, since the primers recognized sequence in PEDF gene while the next primers recognize sequence in ApoE gene. Lanes 15~24: Presence of band (245 bp) indicates ApoE $^{(-/-)}$. Lanes 25: Presence of band (155 bp) indicates ApoE $^{(+/+)}$ (from WT mice as control). (B) Expressions of PEDF protein in ApoE$^{-/-}$ mice (number 1~4) and ApoE$^{-/-}$/PEDF$^{-/-}$ mice (number 5~8) were detected in mouse liver by western blot. (C) Serum PEDF level was measured in WT, ApoE$^{-/-}$, PEDF$^{-/-}$ and ApoE$^{-/-}$/PEDF$^{-/-}$ mice (per group n=5~6) with 8 weeks CD by ELISA. Data are presented as mean ± SEM. ***$P<0.001$ vs ApoE$^{-/-}$/PEDF$^{-/-}$; ###$P<0.001$ vs PEDF$^{-/-}$; &$P<0.05$ vs ApoE$^{-/-}$. DKO indicates double knockout; PCR, polymerase chain reaction; PEDF, pigment epithelial-derived factor; WT, wild type; CD, chow diet; ELISA, enzyme linked immunosorbent assay; SEM, standard error of the mean.

Figure S2. Evaluation of AAV-mediated PEDF expression in ApoE$^{-/-}$/PEDF$^{-/-}$ mice.

(A) An overview of AAV injection process: six to eight weeks old male ApoE$^{-/-}$/PEDF$^{-/-}$ mice were injected either AAV-PEDF or AAV-GFP at 20-week HFD and harvested until 36-week HFD. Age-matched ApoE$^{-/-}$/PEDF$^{-/-}$ with non-injection mice served as blank controls. (B)Representative images of fluorescence intensity in liver and adipose tissue were shown in AAV-CON, AAV-GFP, and AAV-PEDF mice. (C) Western blot analysis was shown the PEDF expressions in liver and adipose tissue (per group n=3). AAV indicates adeno-associated virus; GFP, green fluorescent protein; CON, control; PEDF, pigment epithelial-derived factor; HFD, high-fat diet.

Figure S3. PEDF significantly improves vascular function in condition of hyperlipidemic.
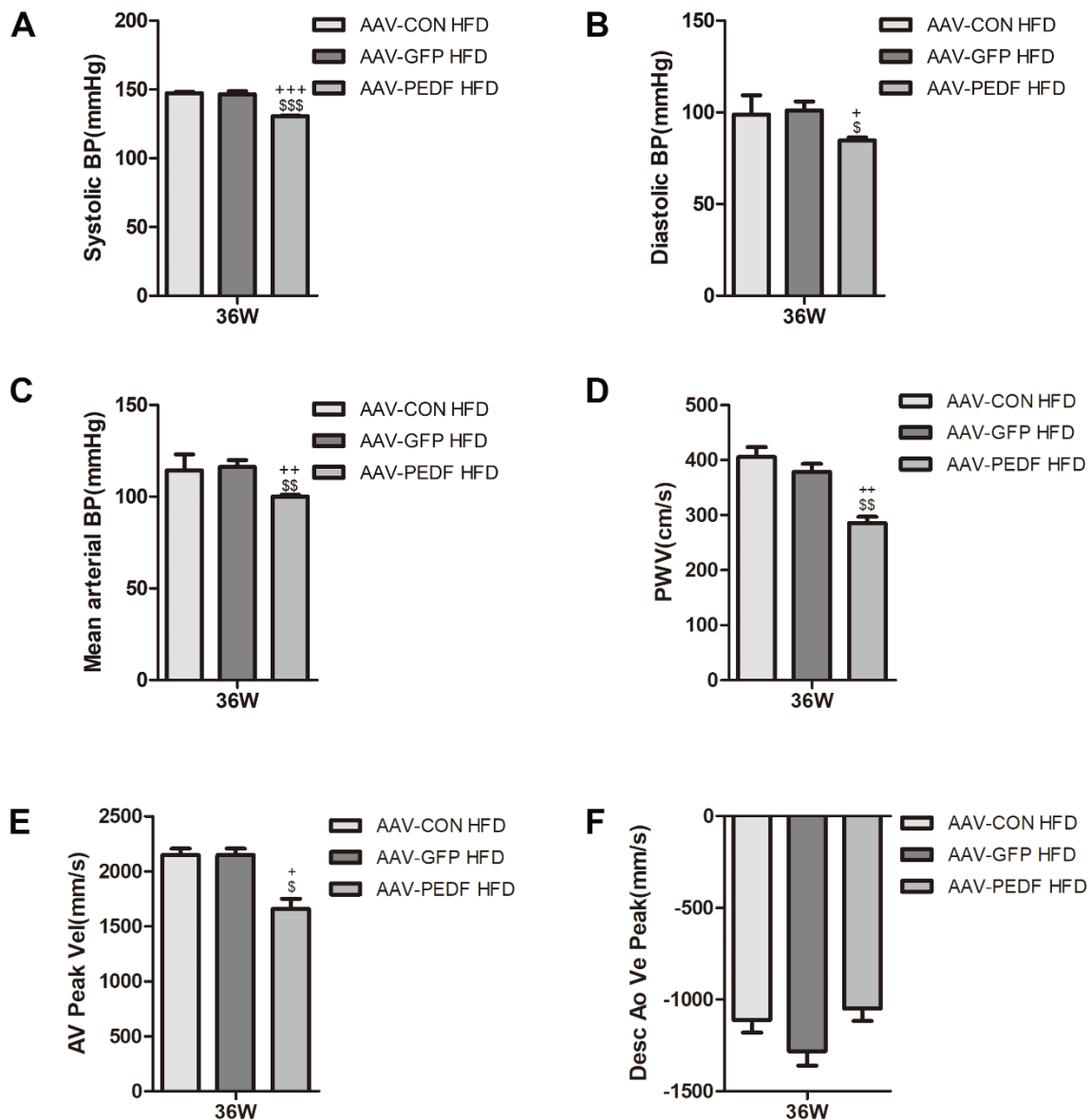
(A) Systolic blood pressure, (B) diastolic blood pressure, and (C) mean arterial blood pressure were measured in AAV-CON, AAV-GFP, and AAV-PEDF mice with 36 weeks HFD (per group n=6~10). (D) Aortic stiffness was assessed by pulse-wave velocity, (E) ascending aortic peak velocity, and (F) descending aortic peak velocity (representative images (left) and quantification (right)) in each group of mice (per group n=4~6). Data are presented as mean ± SEM. $^{\$}P<0.05$, $^{\$\$}P<0.01$, $^{\$\$\$}P<0.001$ vs AAV-CON; $^{+}P<0.05$, $^{++}P<0.01$, $^{+++}P<0.001$ vs AAV-GFP. AAV indicates adeno-associated virus; GFP, green fluorescent protein; CON, control; PEDF, pigment epithelial-derived factor; HFD, high-fat diet; SEM, standard error of the mean.